Simulations of star formation using frequency-dependent radiative transfer

Neil Vaytet

Centre de Recherche Astrophysique de Lyon, ENS Lyon, France

Gilles Chabrier (ENS Lyon)
Matthias González (Paris VII)
Jacques Masson (ENS Lyon)
Edouard Audit (CEA Saclay)
Benoît Commerçon (ENS Paris)

ASTRONUM - Biarritz - 4 July 2013

Background image credit: NASA, ESA, N. Smith et al., and The Hubble Heritage Team (STScI/AURA)

Outline

1. Introduction to star formation
2. Description of the multigroup model for radiation hydrodynamics
3. Simulations of star formation: the first and second collapse
4. Early 3D results with RAMSES
5. Conclusions

Credit: NASA, ESA and J. M. Apellániz (IAA, Spain)

Star formation

- Theory of star formation

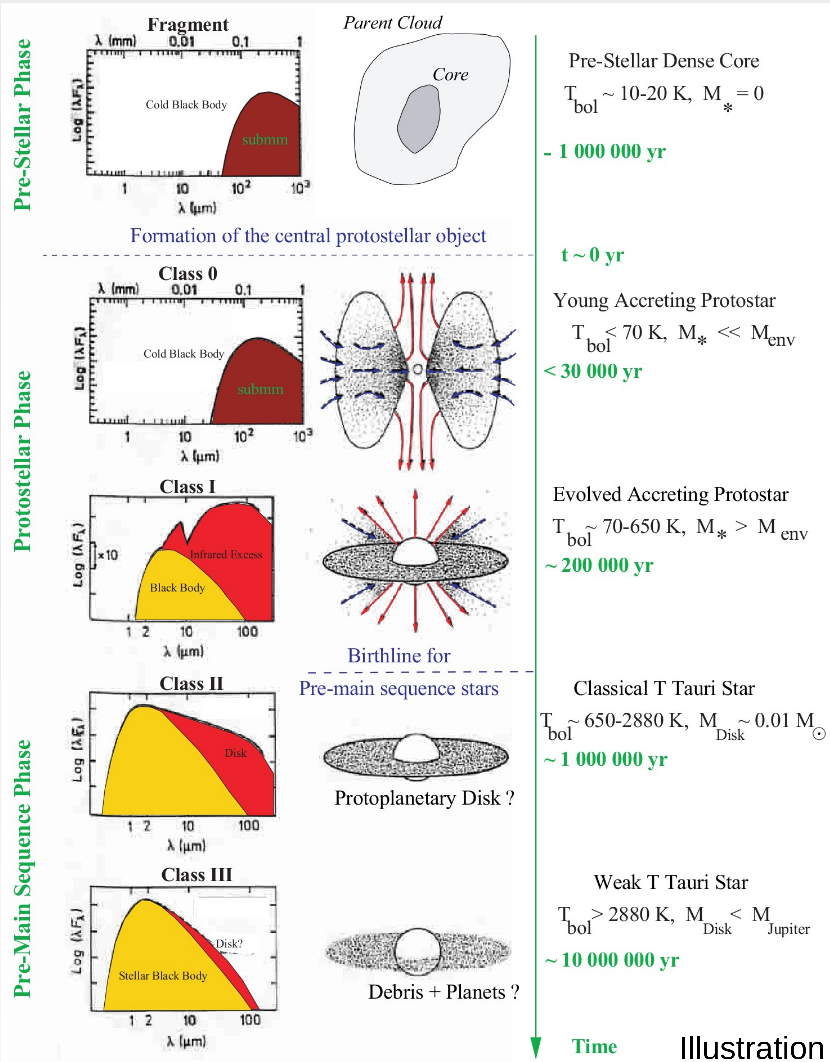

Illustration credits: Andre 2002

Star formation

- Theory of star formation

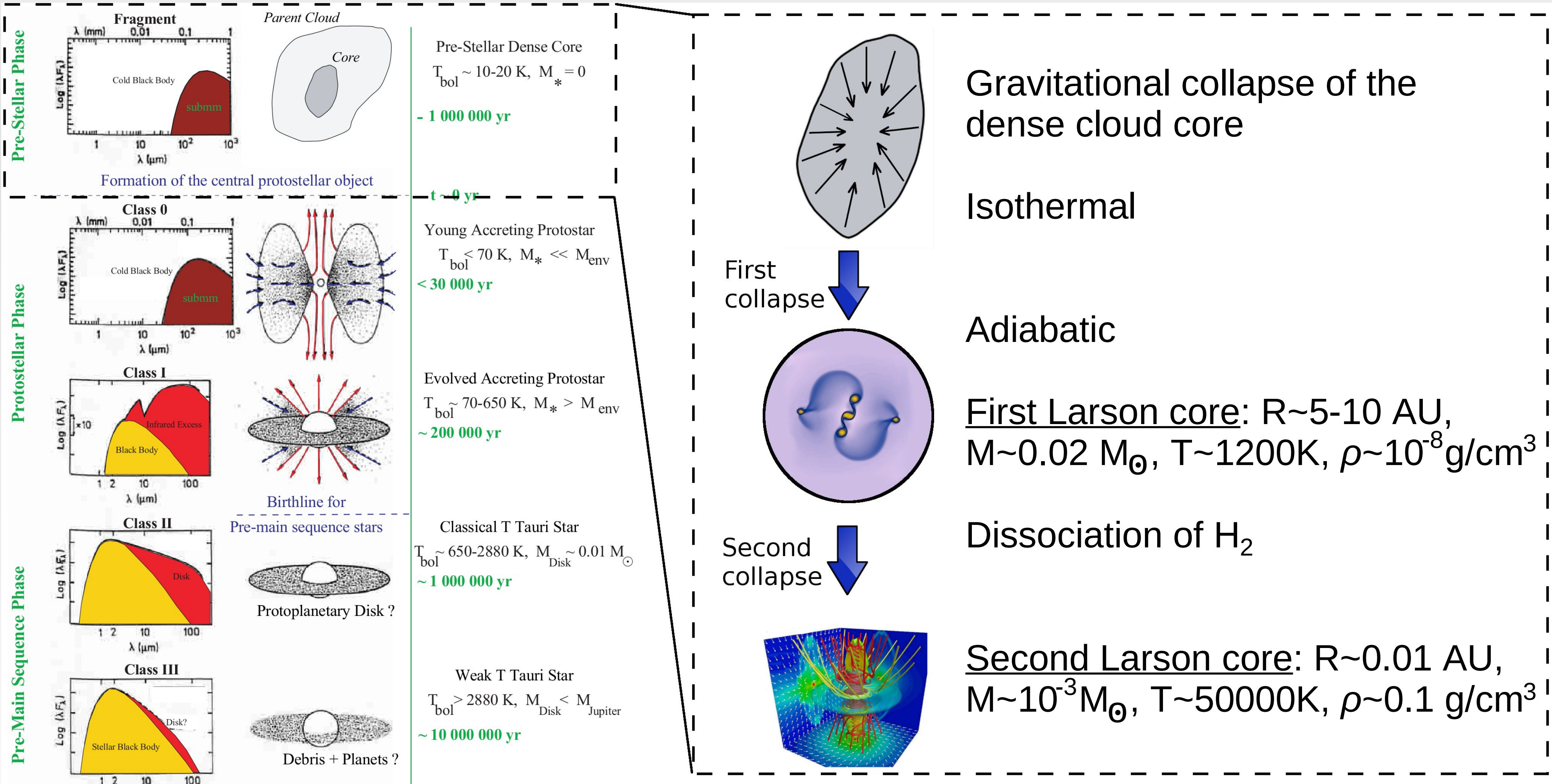

Illustration credits: Andre 2002, Commercon 2010, Tomida et al. 2011

Star formation

▪ Current problems in star formation

- Observed spread in luminosities suggests that star formation could be a lengthy process

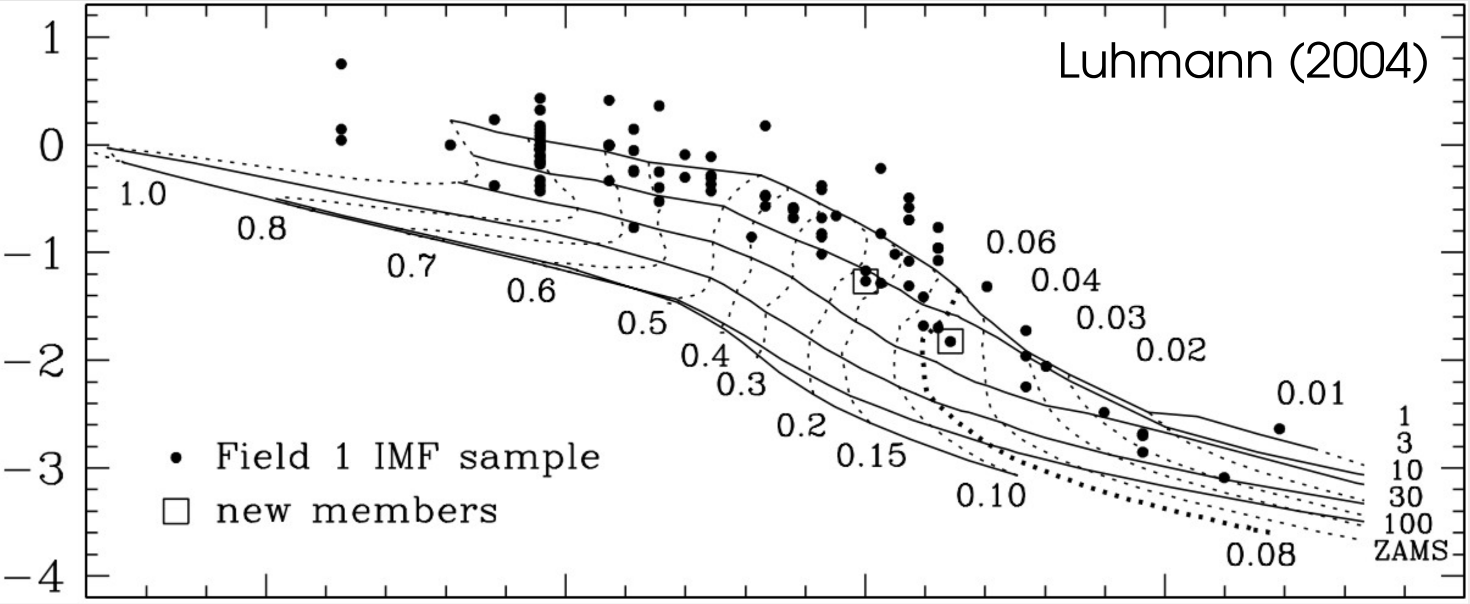

- Isochrones span several million years

$$t_{ff} = \frac{1}{4}\sqrt{\frac{3\pi}{2G\rho}} \simeq 180,000 \text{ yrs}$$

- The free fall time for a 1 M⊙ cloud of size 10,000 AU is smaller by an order of magnitude
- Star formation takes several million years?
- Episodic accretion? (Baraffe et al. 2009; 2012; see also Patrick Lii's talk)

Star formation

▪ Current problems in star formation

The importance of radiative transfer:

- The inefficiency of star formation: observed star formation rates are difficult to reproduce with numerical simulations.
- Radiative transfer can strongly inhibit fragmentation in collapsing clouds (Price & Bate 2009; Offner et al. 2009; Commercon et al. 2010)

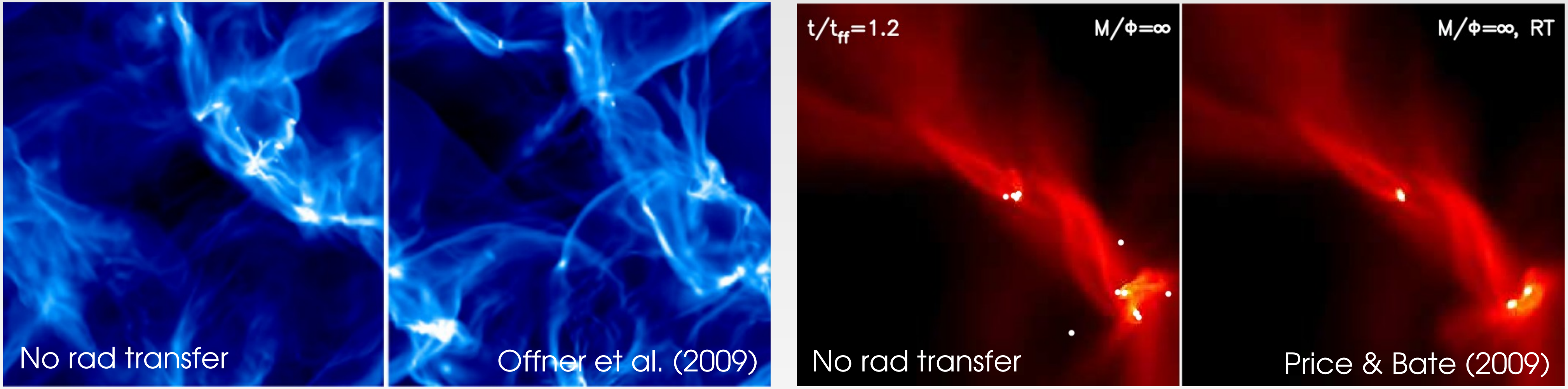

- Simulations make use of grey approximations and Flux Limited Diffusion for the radiative transfer.

Radiative transfer

- See Matthias González's talk

Why use multigroup?

- The gas and dust opacities are absolutely crucial to radiative transfer

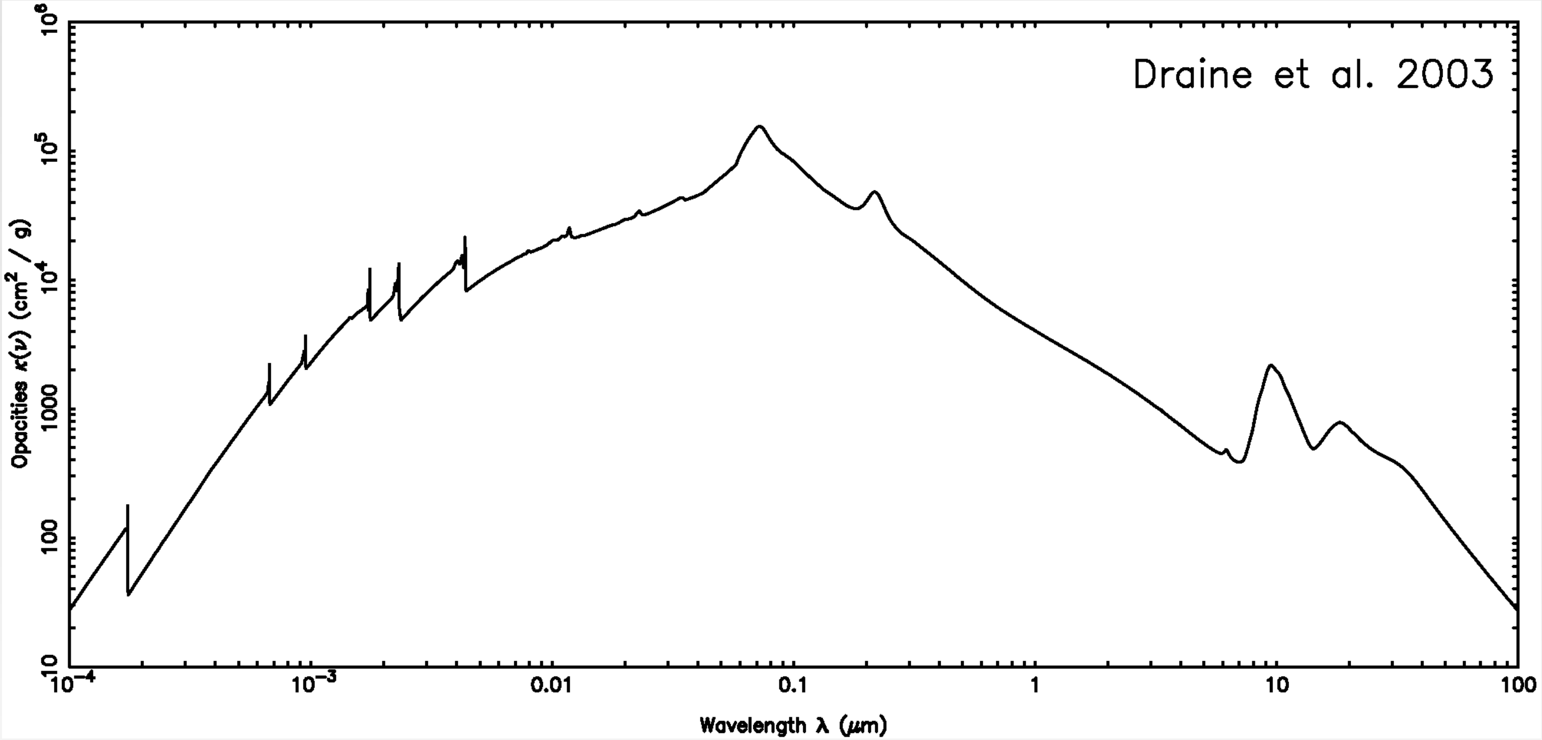

Radiative transfer

Why use multigroup?

- The gas and dust opacities are absolutely crucial to radiative transfer

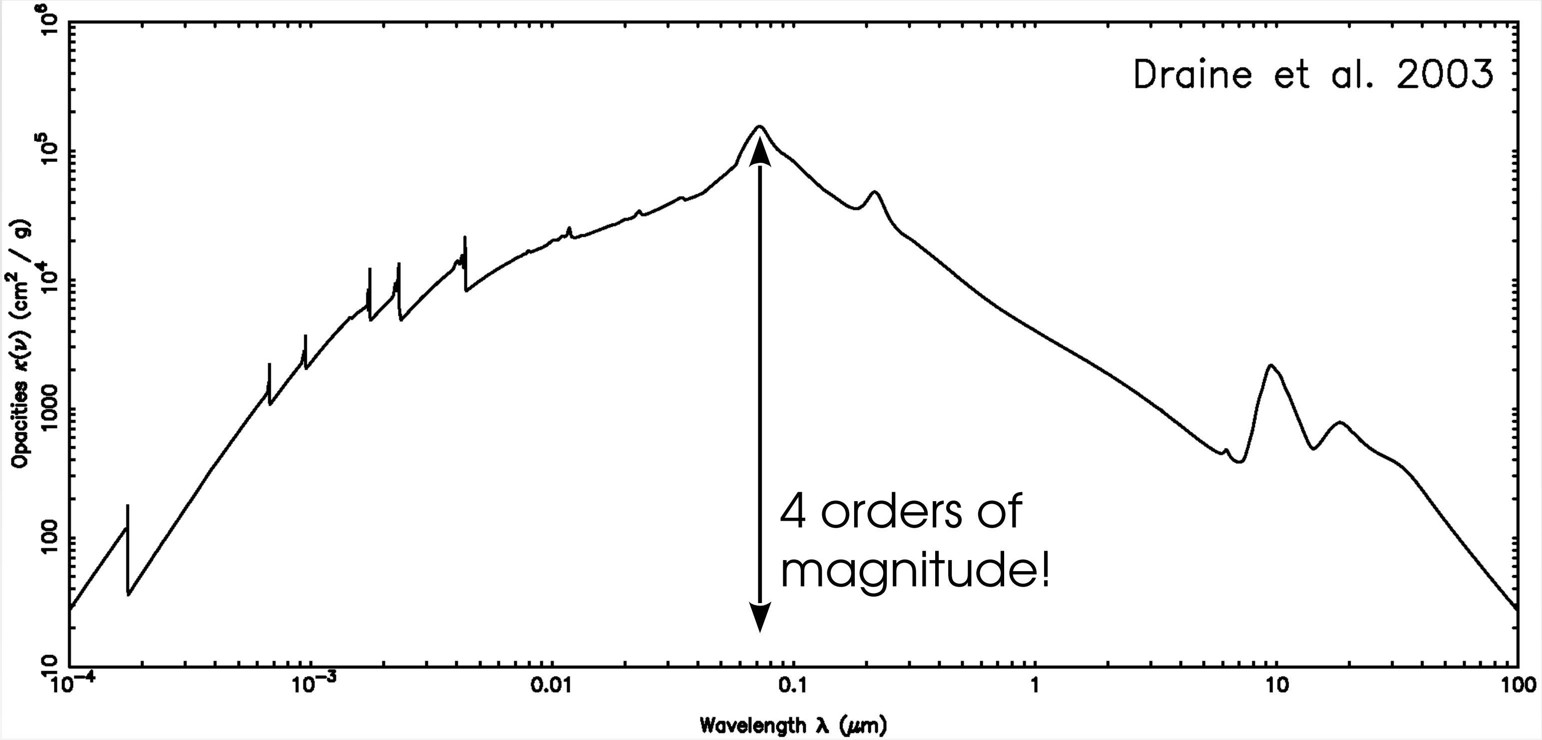

Radiative transfer

Why use multigroup?

- The gas and dust opacities are absolutely crucial to radiative transfer

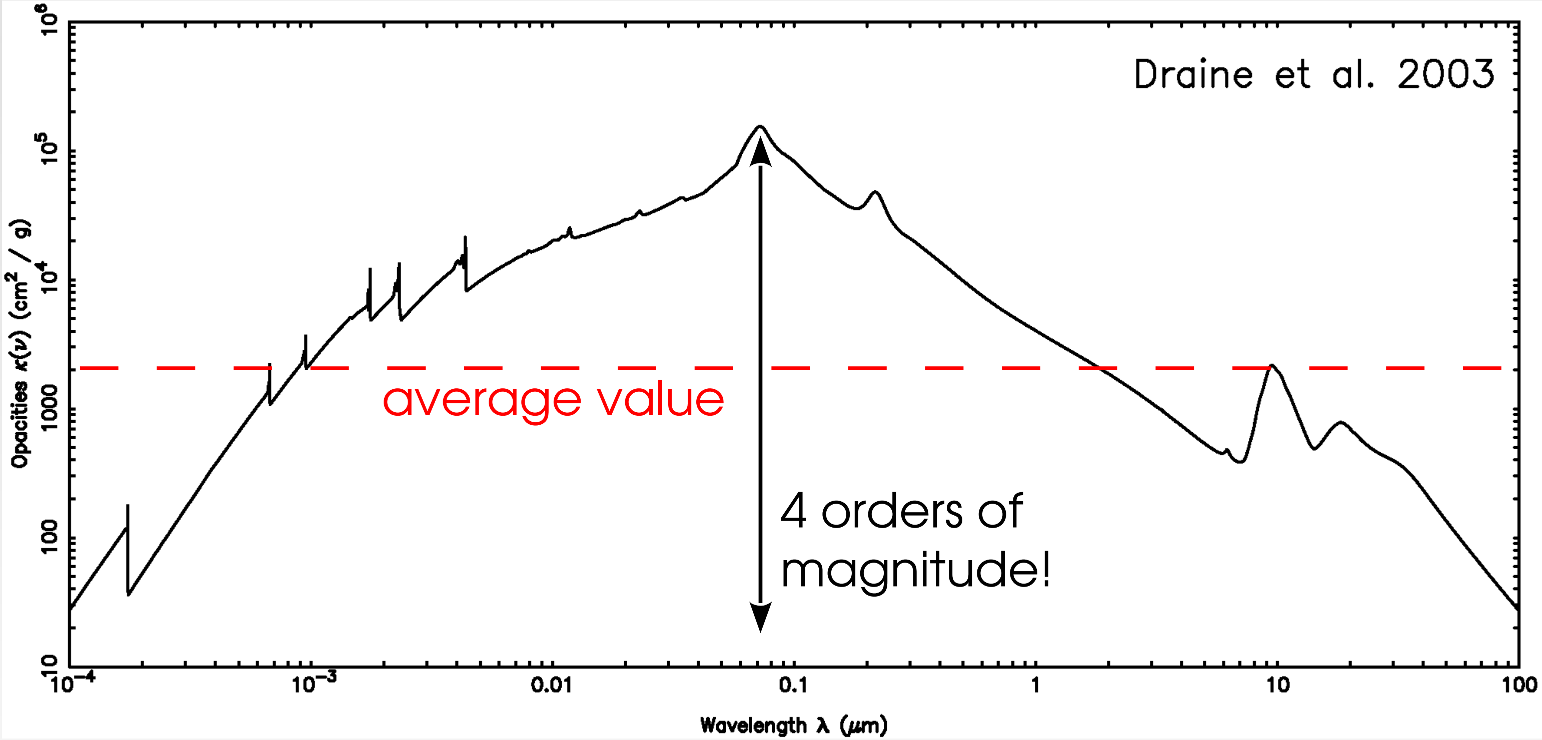

Radiative transfer

Why use multigroup?

- The gas and dust opacities are absolutely crucial to radiative transfer

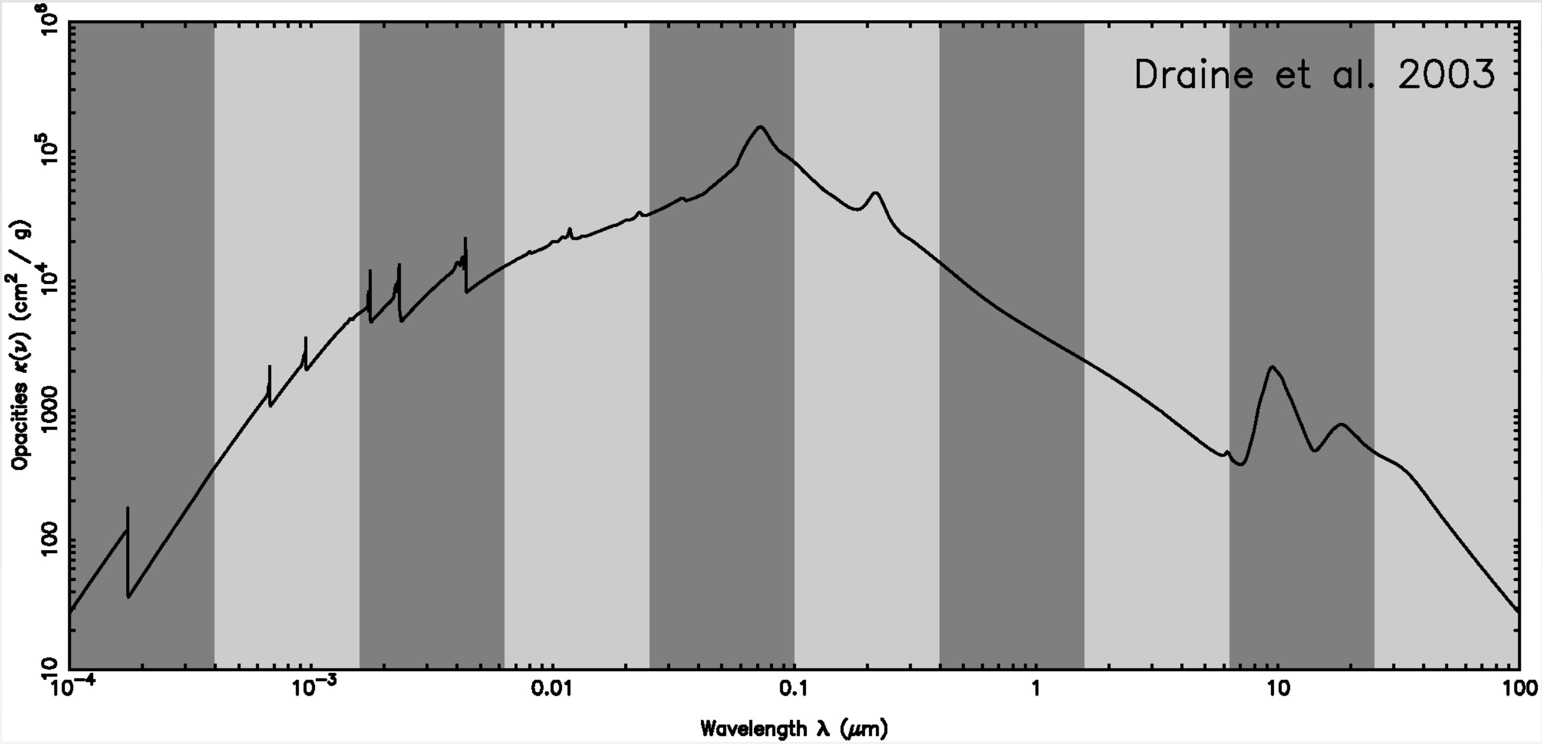

- The multigroup method: split the frequency domain into groups and solve the equations of radiative transfer inside each group.

Radiative transfer

<u>Why use multigroup?</u>

- The gas and dust opacities are absolutely crucial to radiative transfer

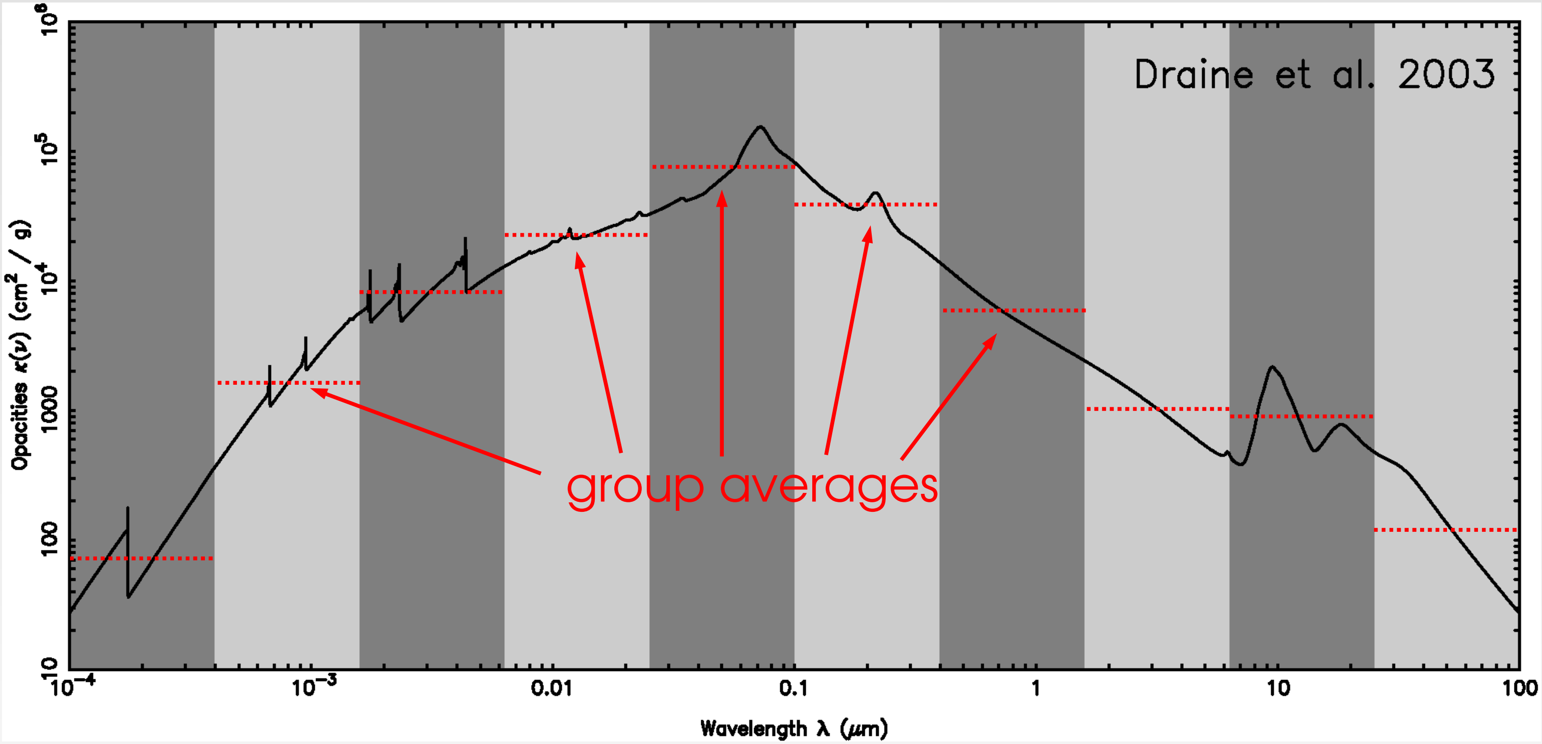

- The multigroup method: split the frequency domain into groups and solve the equations of radiative transfer inside each group.

Radiative transfer

Why use multigroup?

- The gas and dust opacities are absolutely crucial to radiative transfer

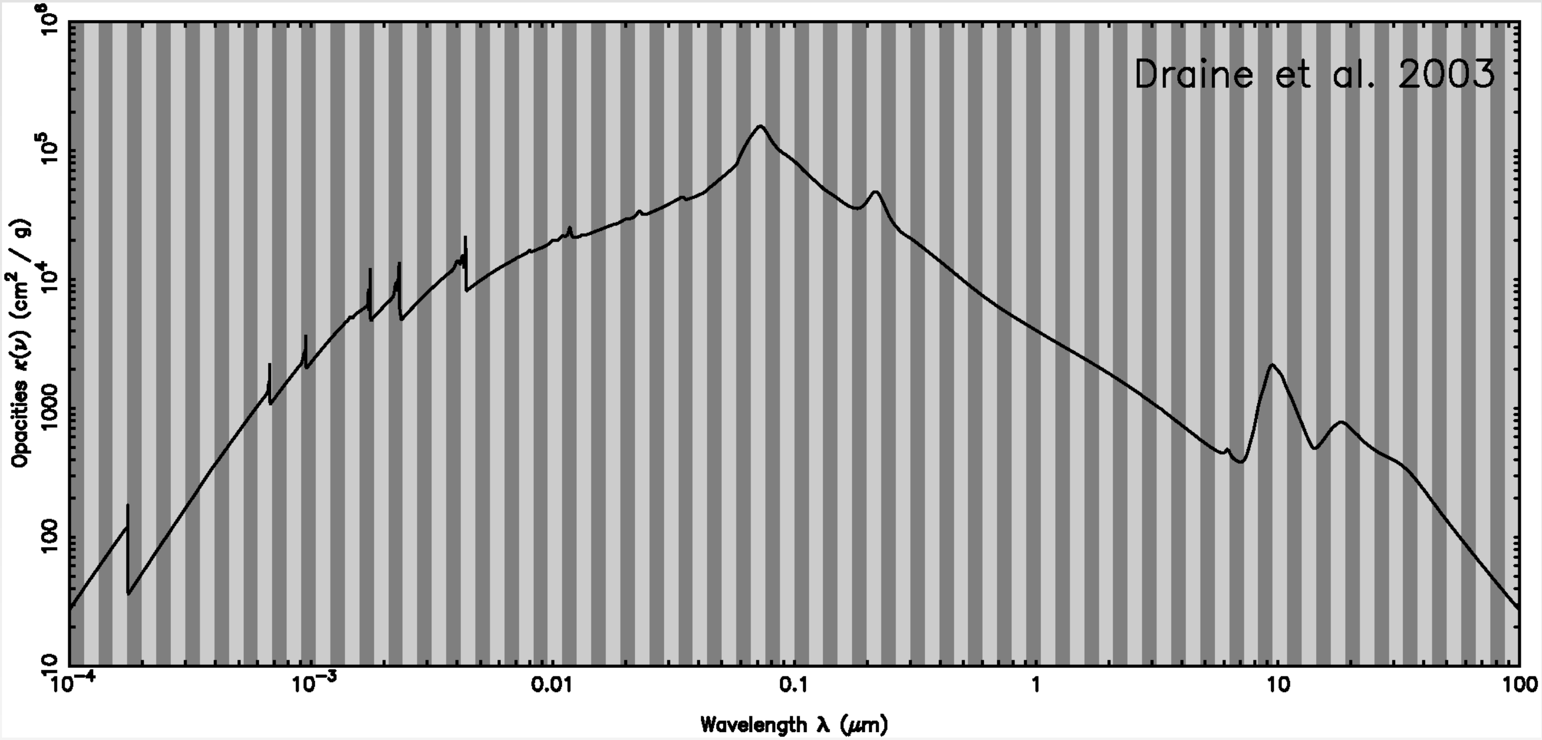

- The multigroup method: split the frequency domain into groups and solve the equations of radiative transfer inside each group.

Numerical method

The SINERGHY1D and HERACLES codes

The SINERGHY1D code:

- Fully implicit 1D MPI-OPENMP Godunov code with 3 possible grid geometries (cartesian, cylindrical, spherical)
- HLLC solver for radiative fluxes
- Matrix inversion using LAPACK

The HERACLES code:

- 3D MPI MHD Godunov code with 3 possible grid geometries (cartesian, cylindrical, spherical)
- Explicit hydrodynamics
- Implicit radiative transfer

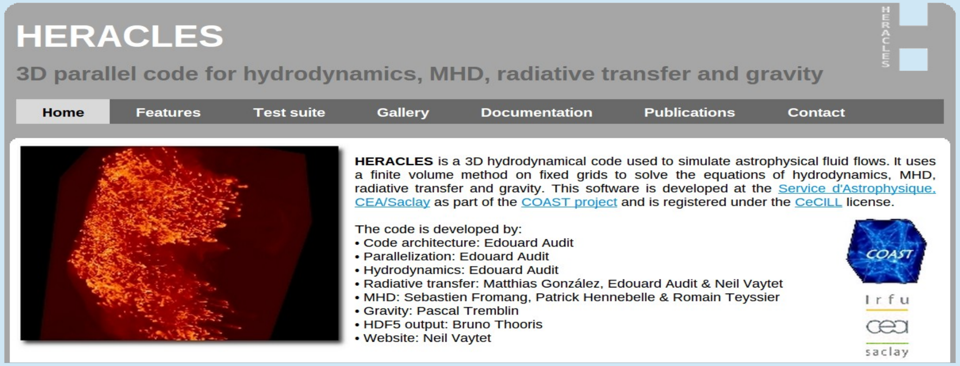

M. González's talk:

- Multigroup simulations of radiative shocks
- Effects on precursor sizes
- Adaptation zones

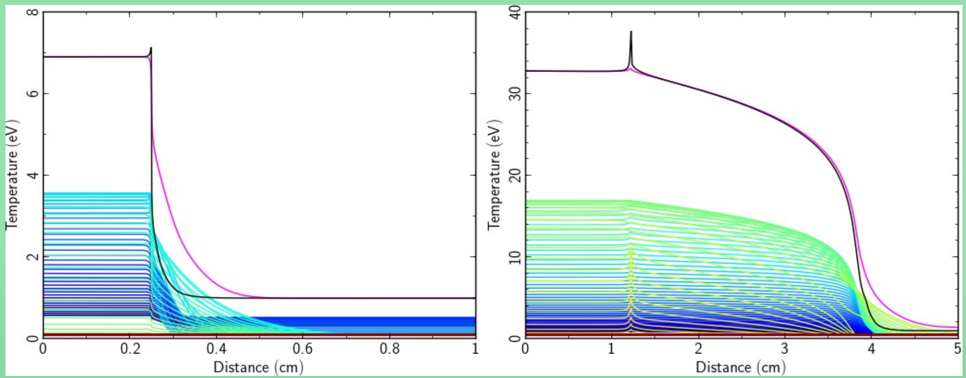

Gravitational collapse using multigroup RHD

▪ Simulation setup

<u>Initial conditions</u>:

- 1 $M_\odot$ uniform ρ cloud with T = 10 K
- Gas and radiation in equilibrium
- R = 10^4 AU
- nz = 2000 cells (log-regular)

<u>Equation of state</u>: Saumon, Chabrier & van Horn (1995)

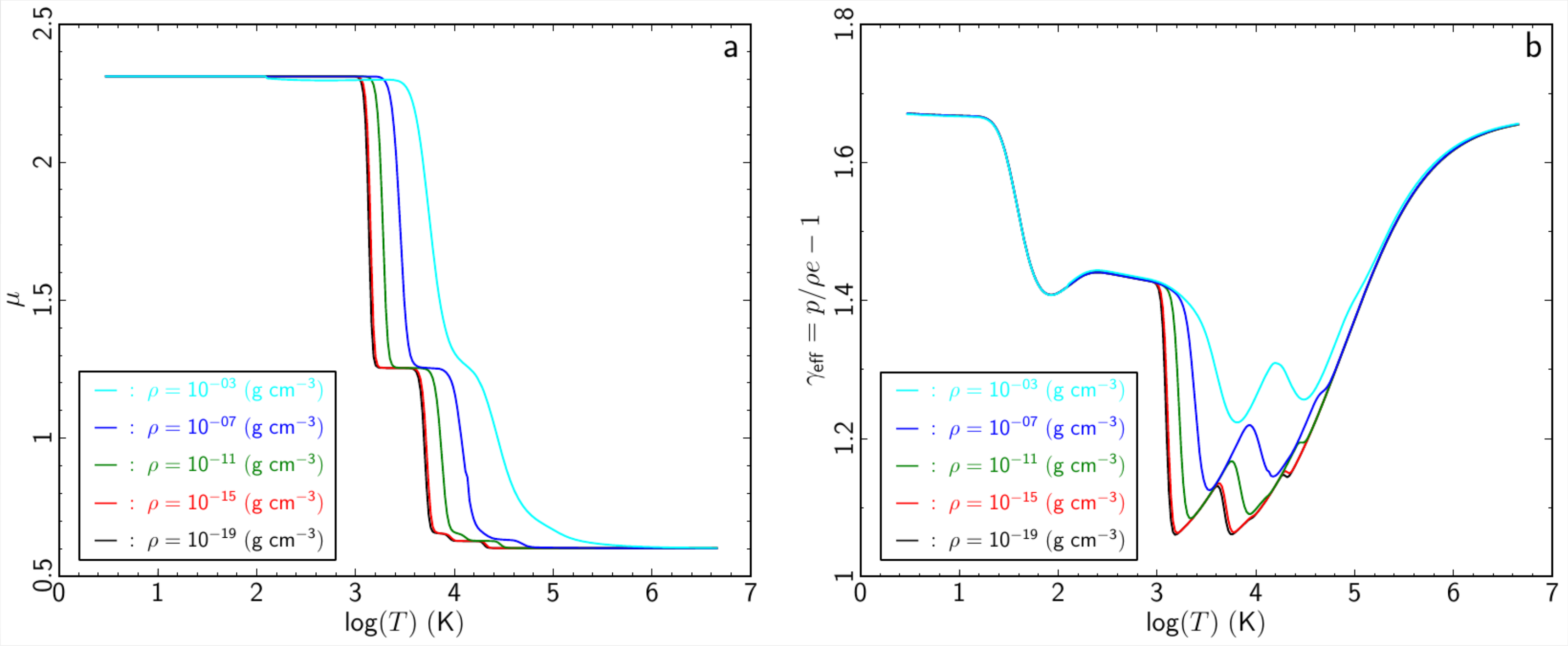

Gravitational collapse using multigroup RHD

- The interstellar dust and gas opacities

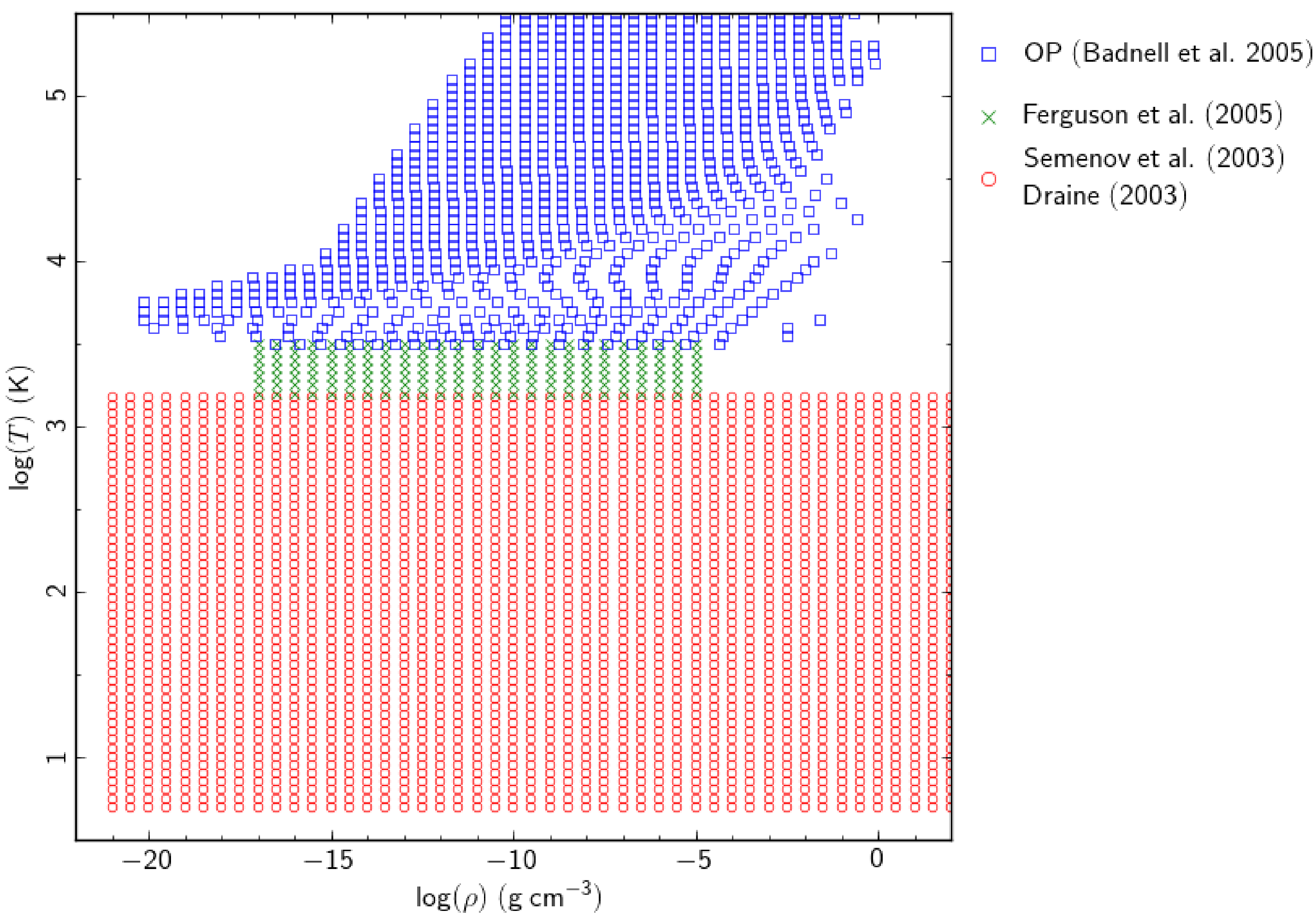

Gravitational collapse using multigroup RHD

- The interstellar dust and gas opacities

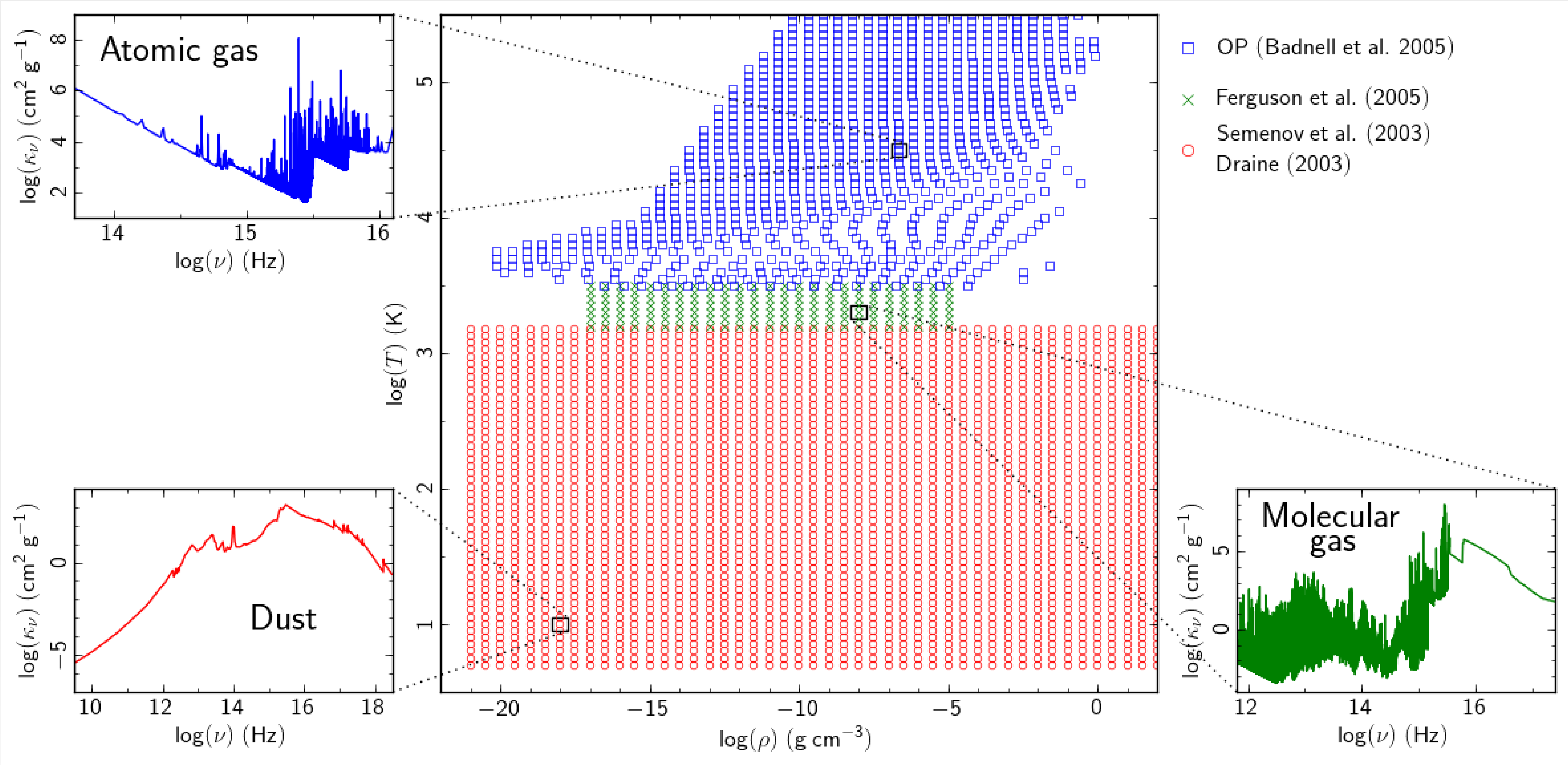

Gravitational collapse using multigroup RHD

- The interstellar dust and gas opacities

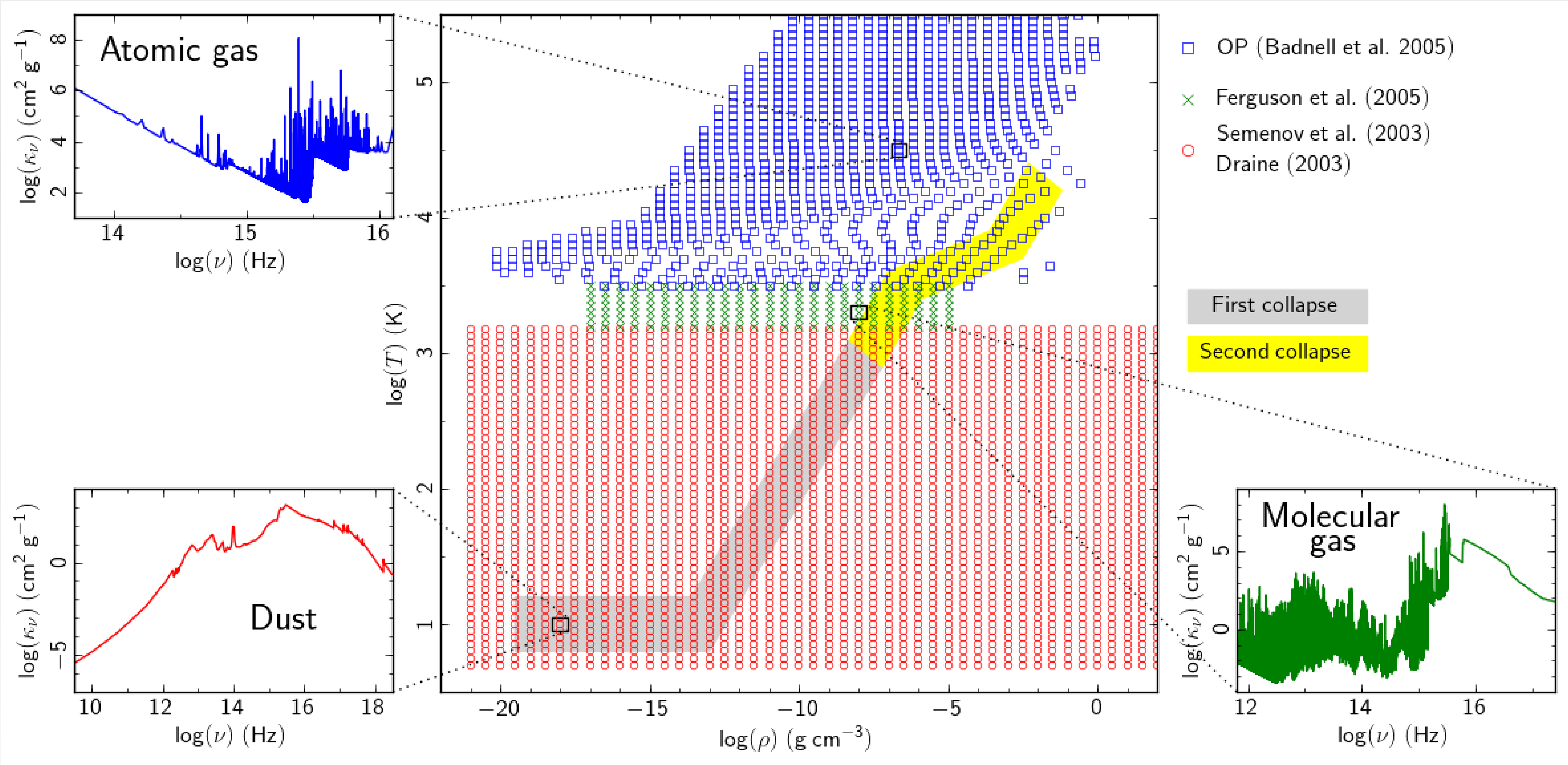

Gravitational collapse using multigroup RHD

- The interstellar dust and gas opacities

Step 1:
Compute opacity in each group for each point in the (ρ , T) plane once at the start of the simulation.

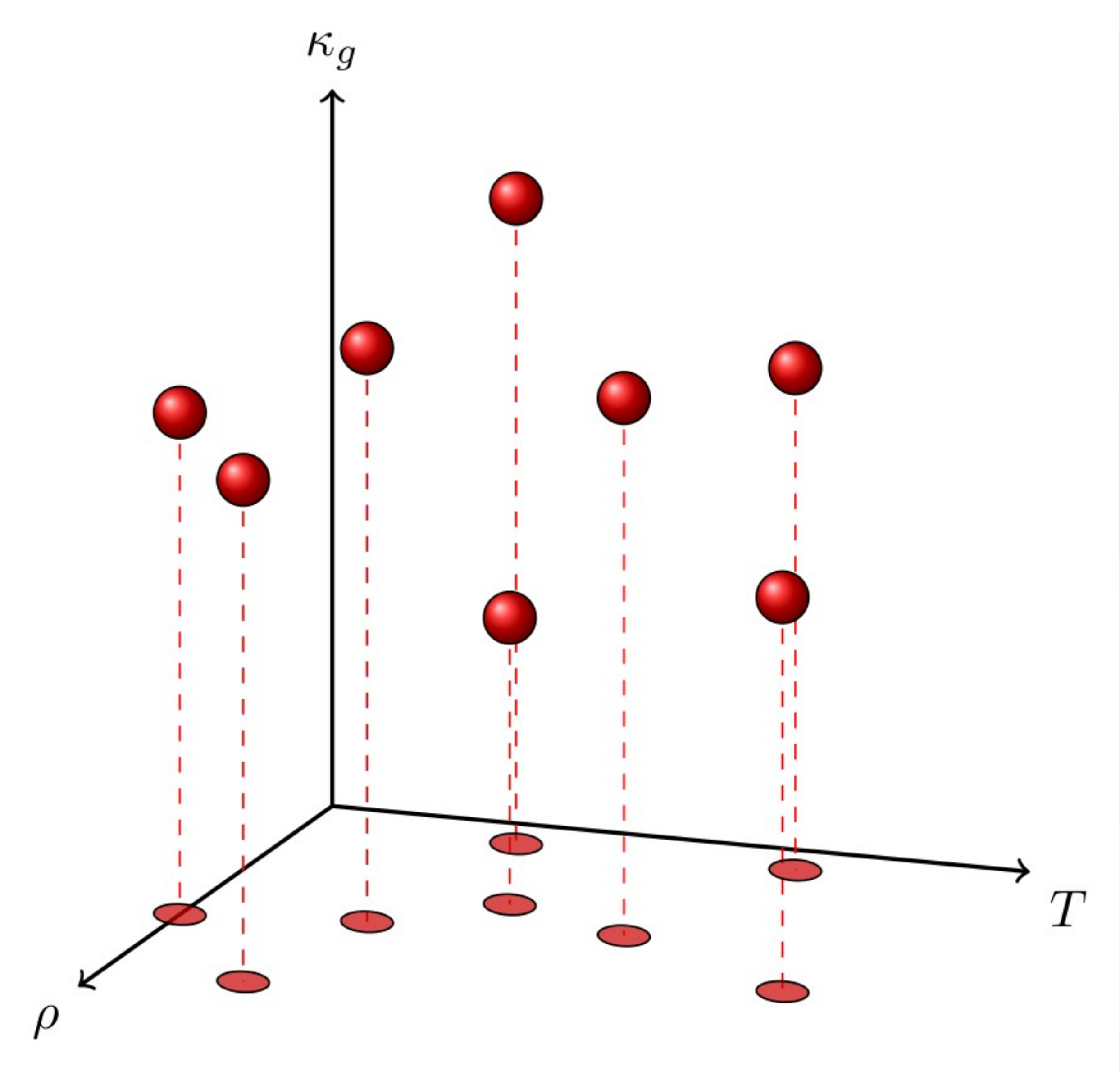

Gravitational collapse using multigroup RHD

- The interstellar dust and gas opacities

Step 2:
Compute Delaunay triangulation in the (ρ , T) plane.

Each triangle represents a plane in the (ρ , T , κ) volume.

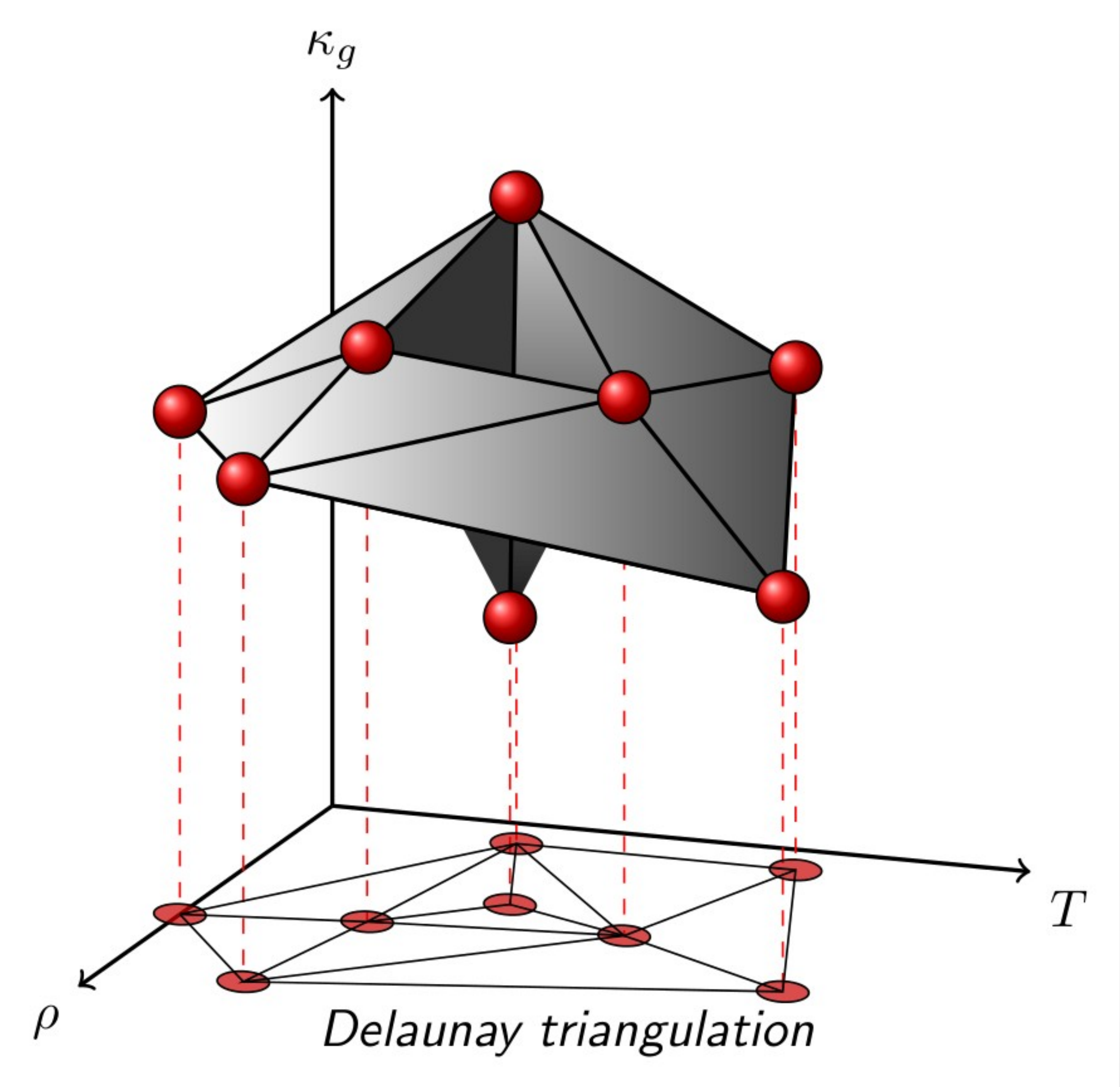

Gravitational collapse using multigroup RHD

- The interstellar dust and gas opacities

<u>Step 3</u>:
Overlay regular mesh onto the computed planes.

This allows for fast index finding during the rest of the simulation.

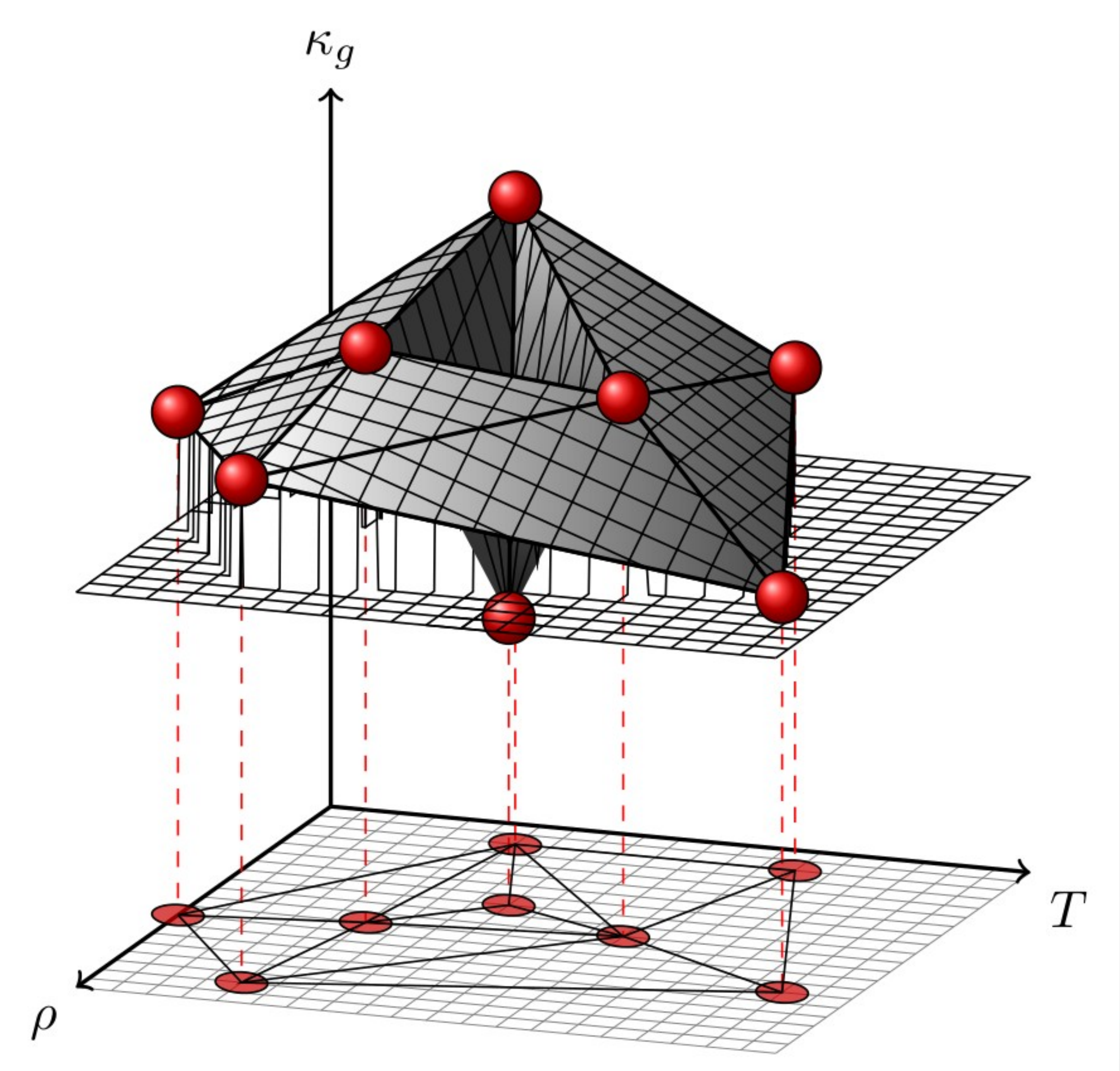

Gravitational collapse using multigroup RHD

- The interstellar dust and gas opacities

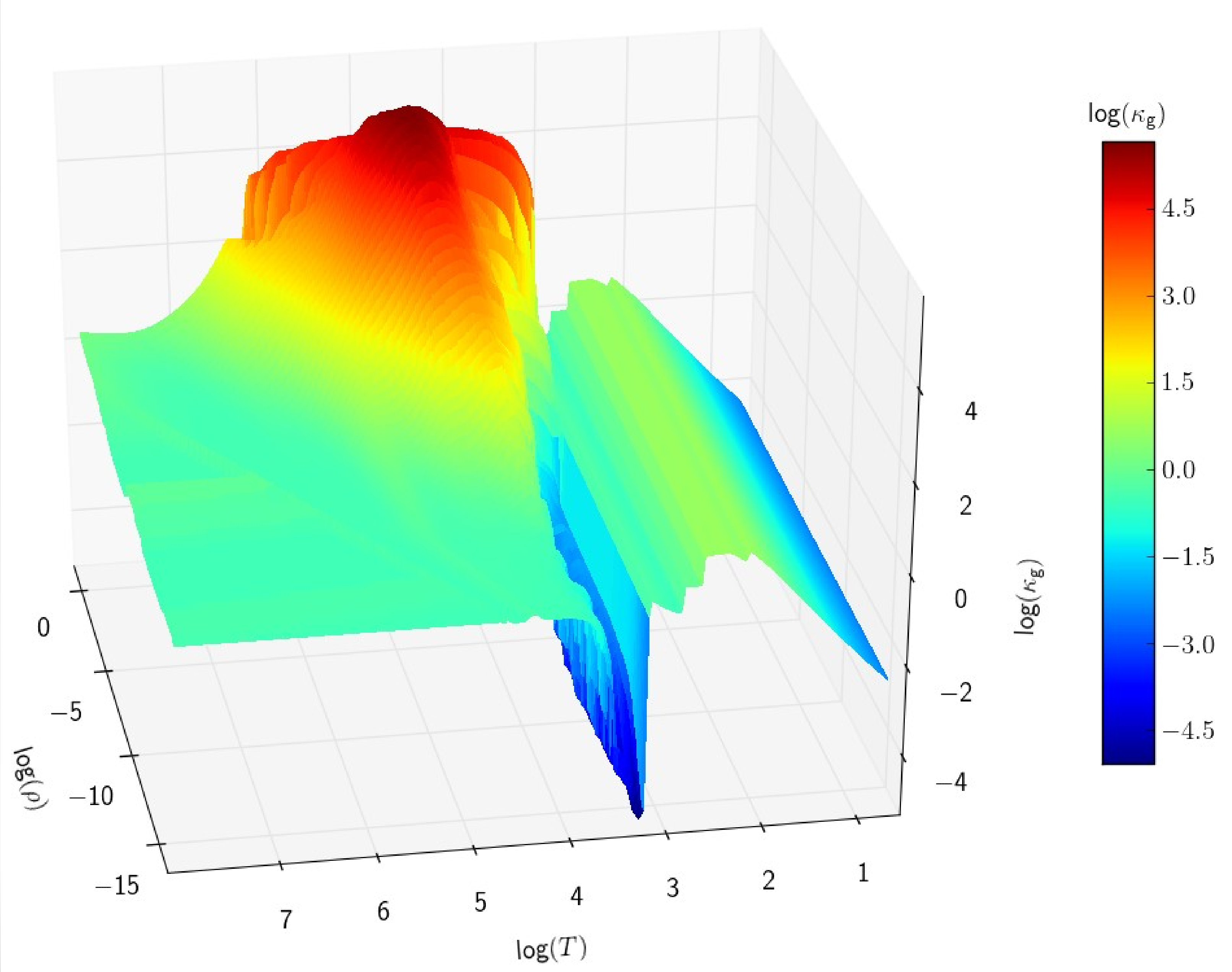

Gravitational collapse using multigroup RHD

- Results: thermal evolution

Vaytet et al. (2013) A&A (acc.)

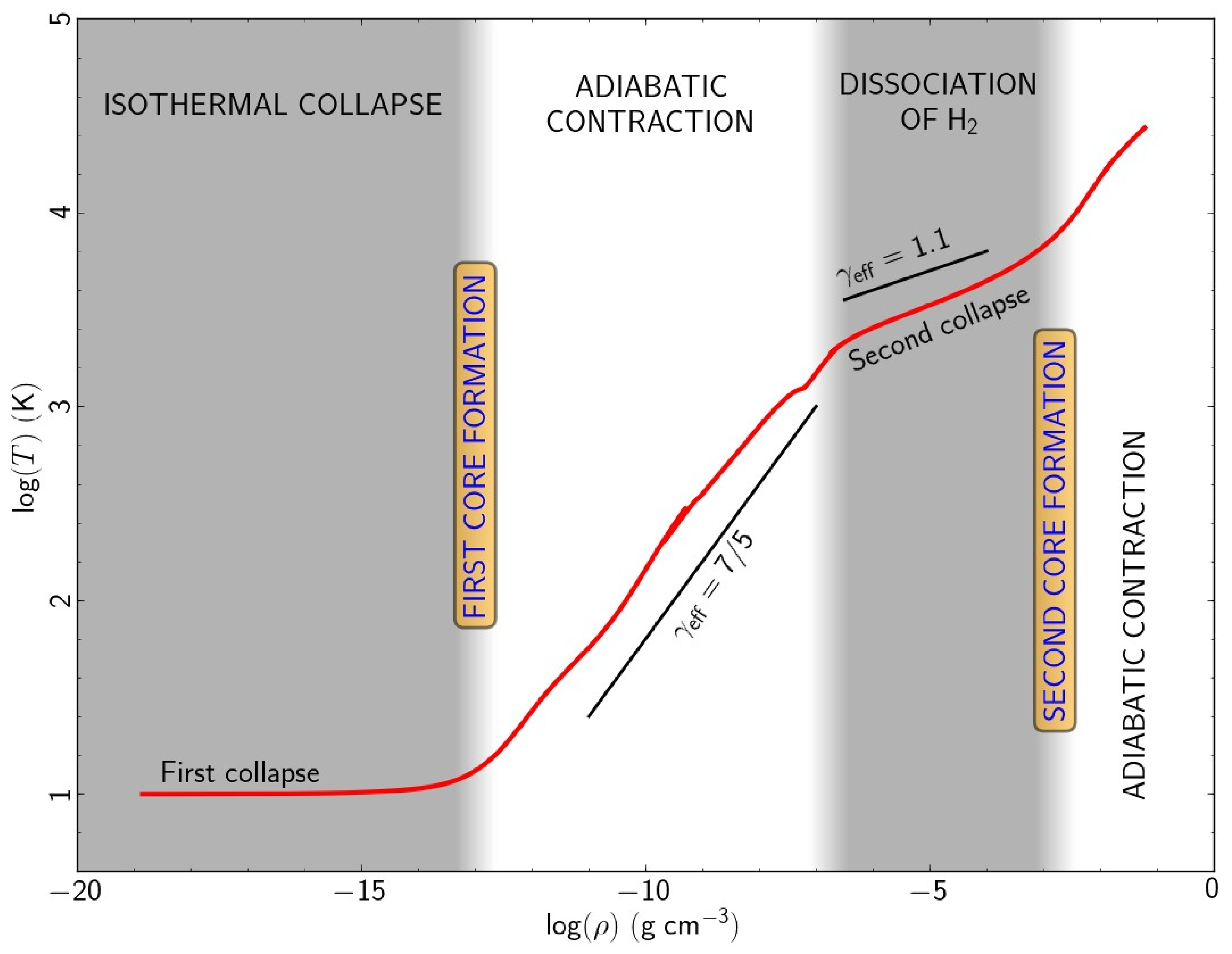

Vaytet et al. A&A (sub.)

Gravitational collapse using multigroup RHD

- Results: thermal evolution

Vaytet et al. (2013) A&A (acc.)

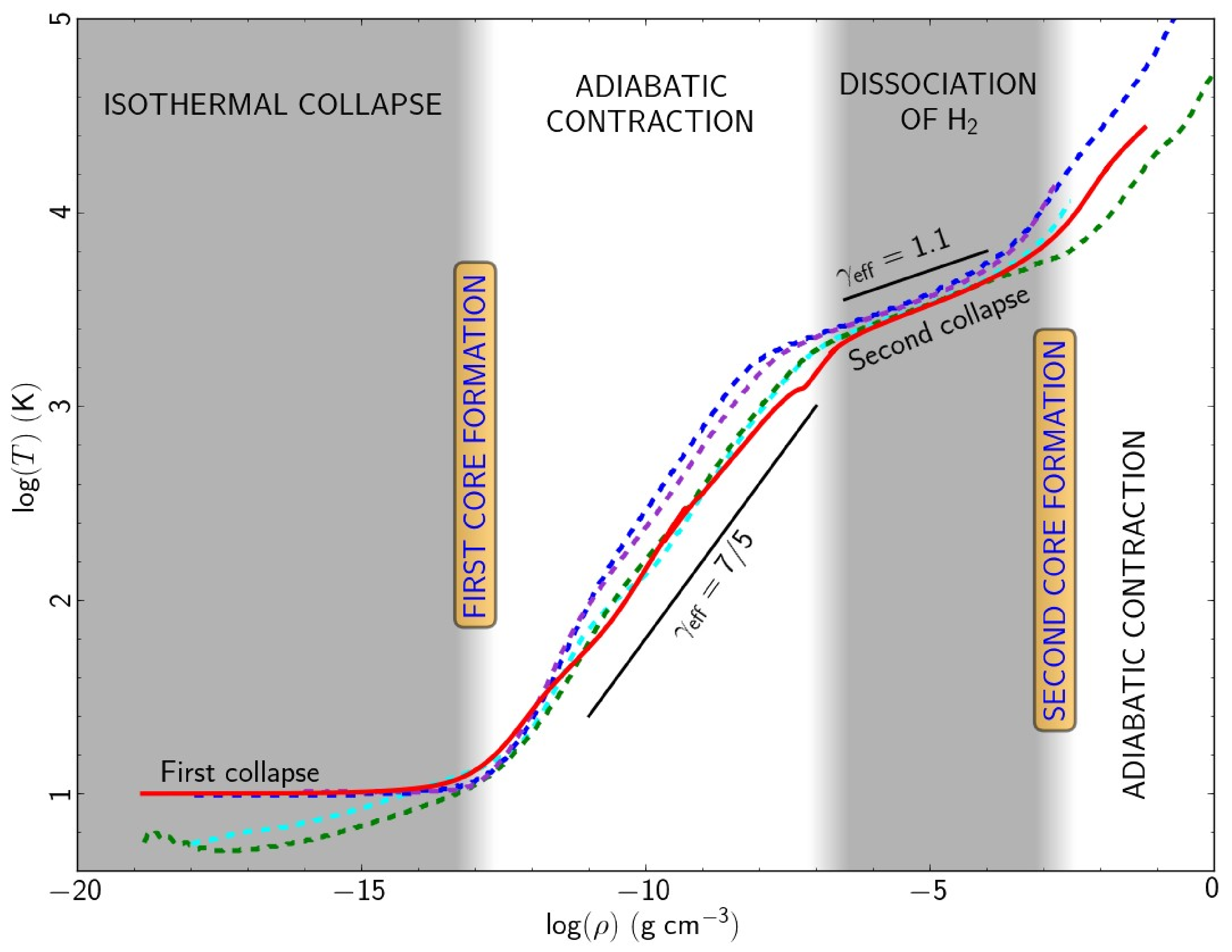

Vaytet et al. A&A (sub.), Masunaga & Inutsuka (2000), Stamatellos et al. (2007), Tomida et al. (2013), Whitehouse & Bate (2006)

Gravitational collapse using multigroup RHD

- Results: thermal evolution

Vaytet et al. (2013) A&A (acc.)

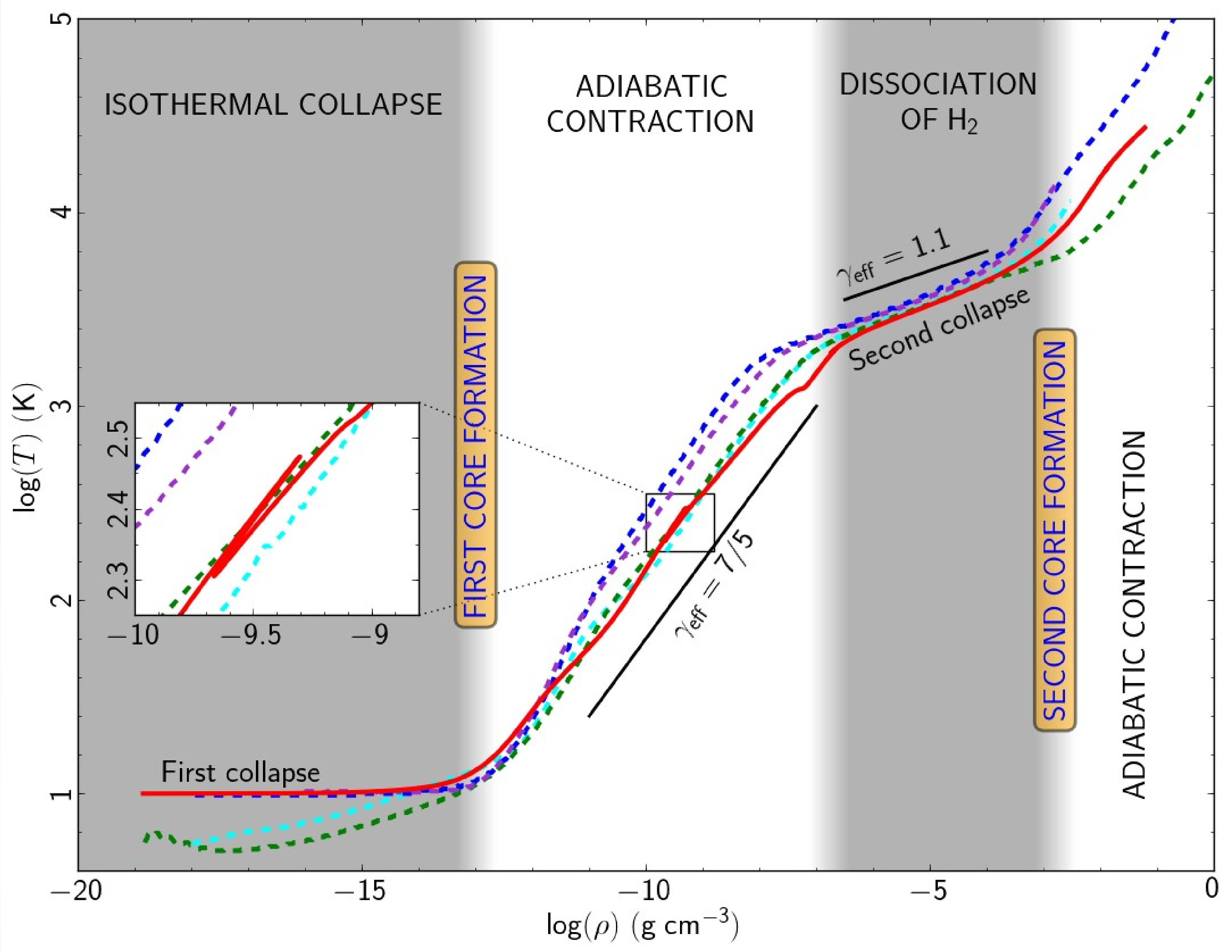

Vaytet et al. A&A (sub.), Masunaga & Inutsuka (2000), Stamatellos et al. (2007), Tomida et al. (2013), Whitehouse & Bate (2006)

Gravitational collapse using multigroup RHD

- Results: radial profiles

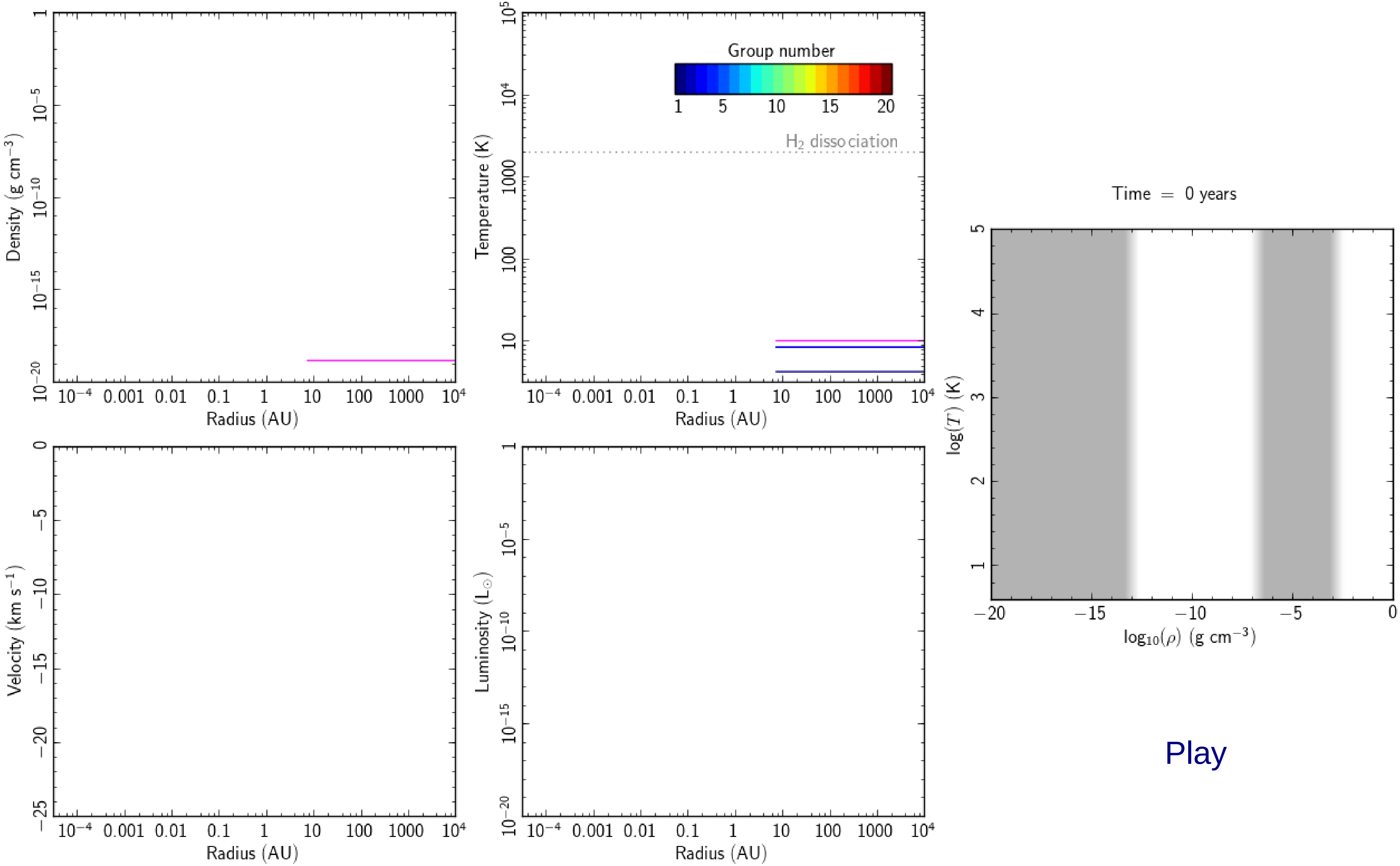

Play

Gravitational collapse using multigroup RHD

- Results: radial profiles

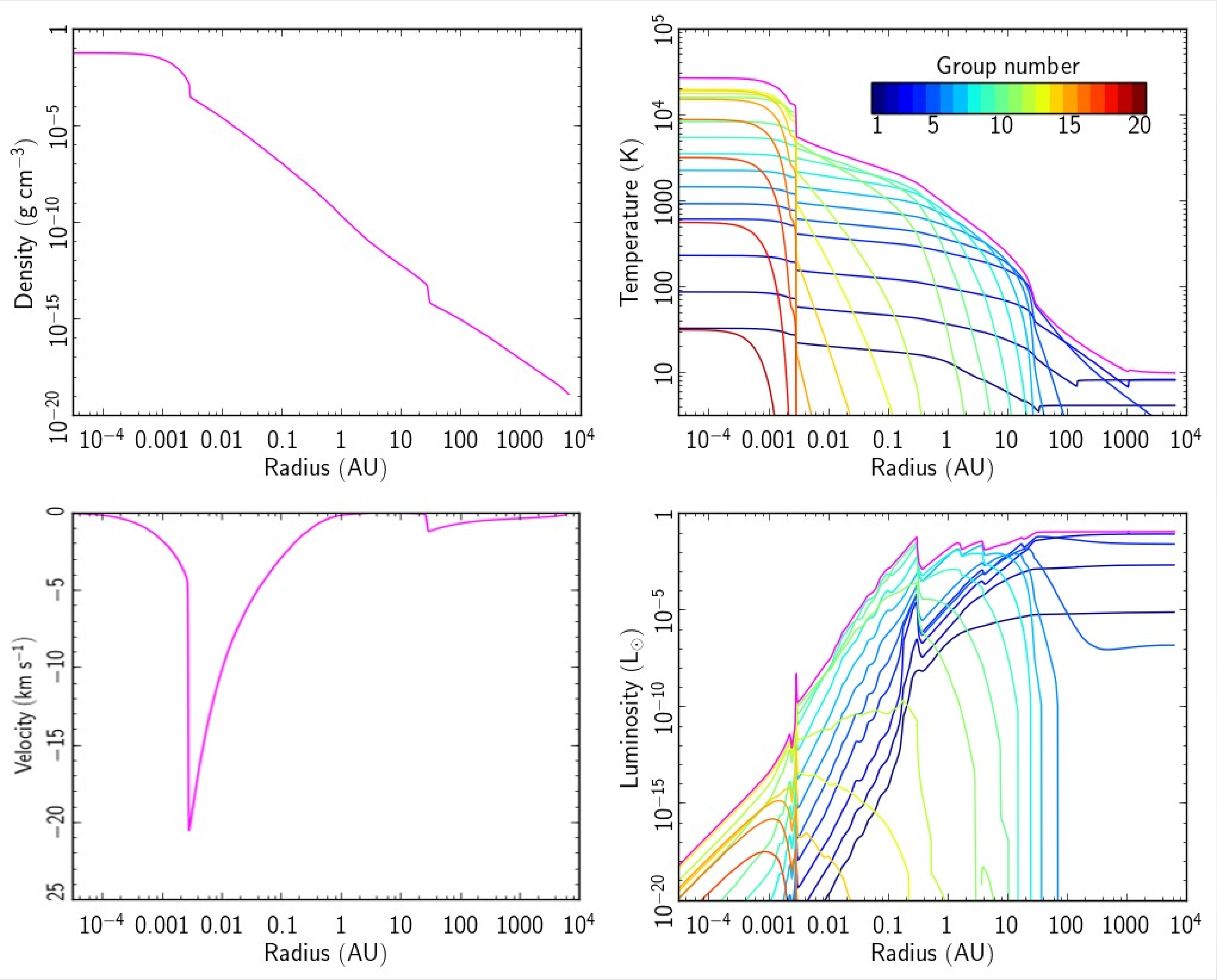

Gravitational collapse using multigroup RHD

- Results: radial profiles

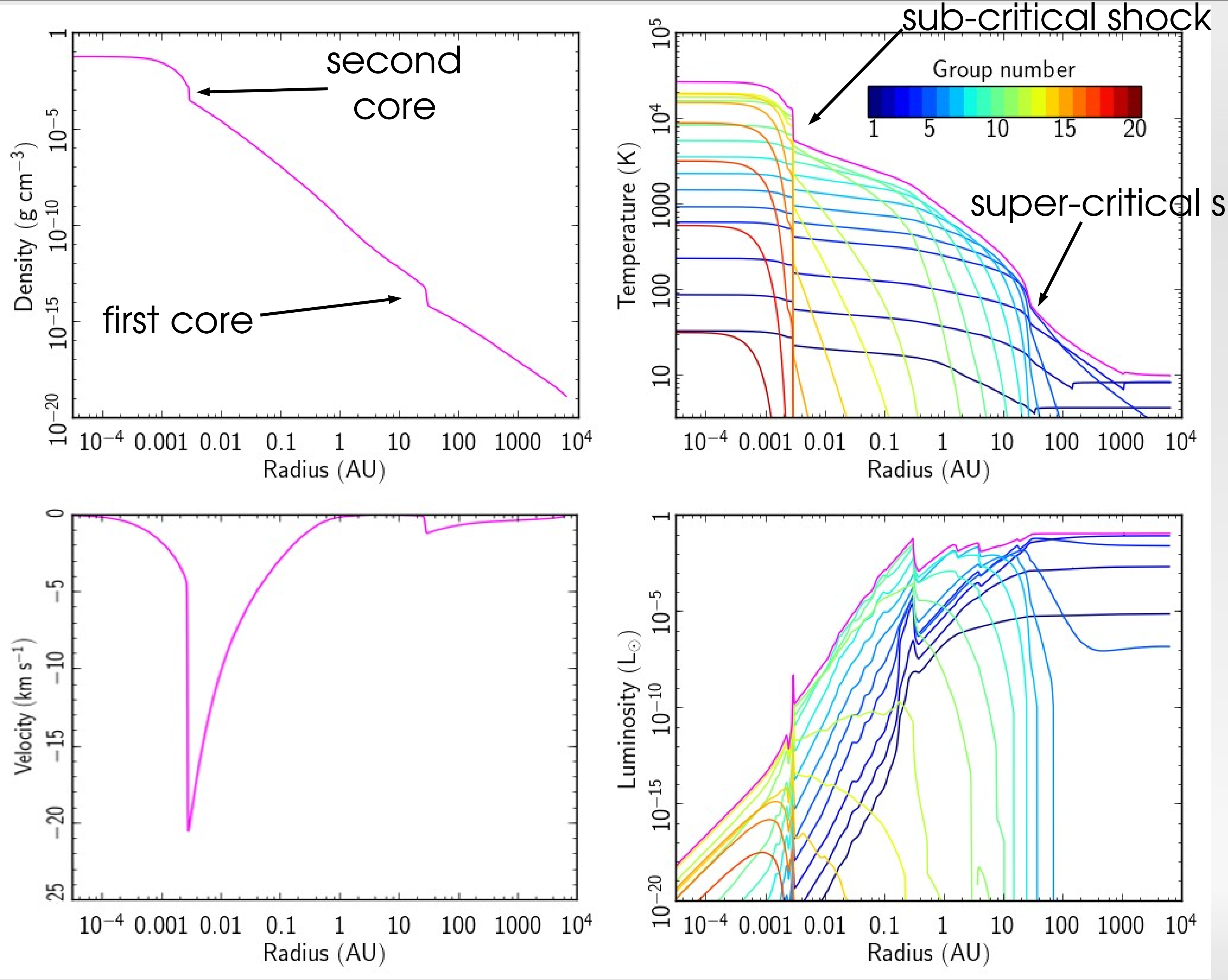

Gravitational collapse using multigroup RHD

- Results: radial profiles

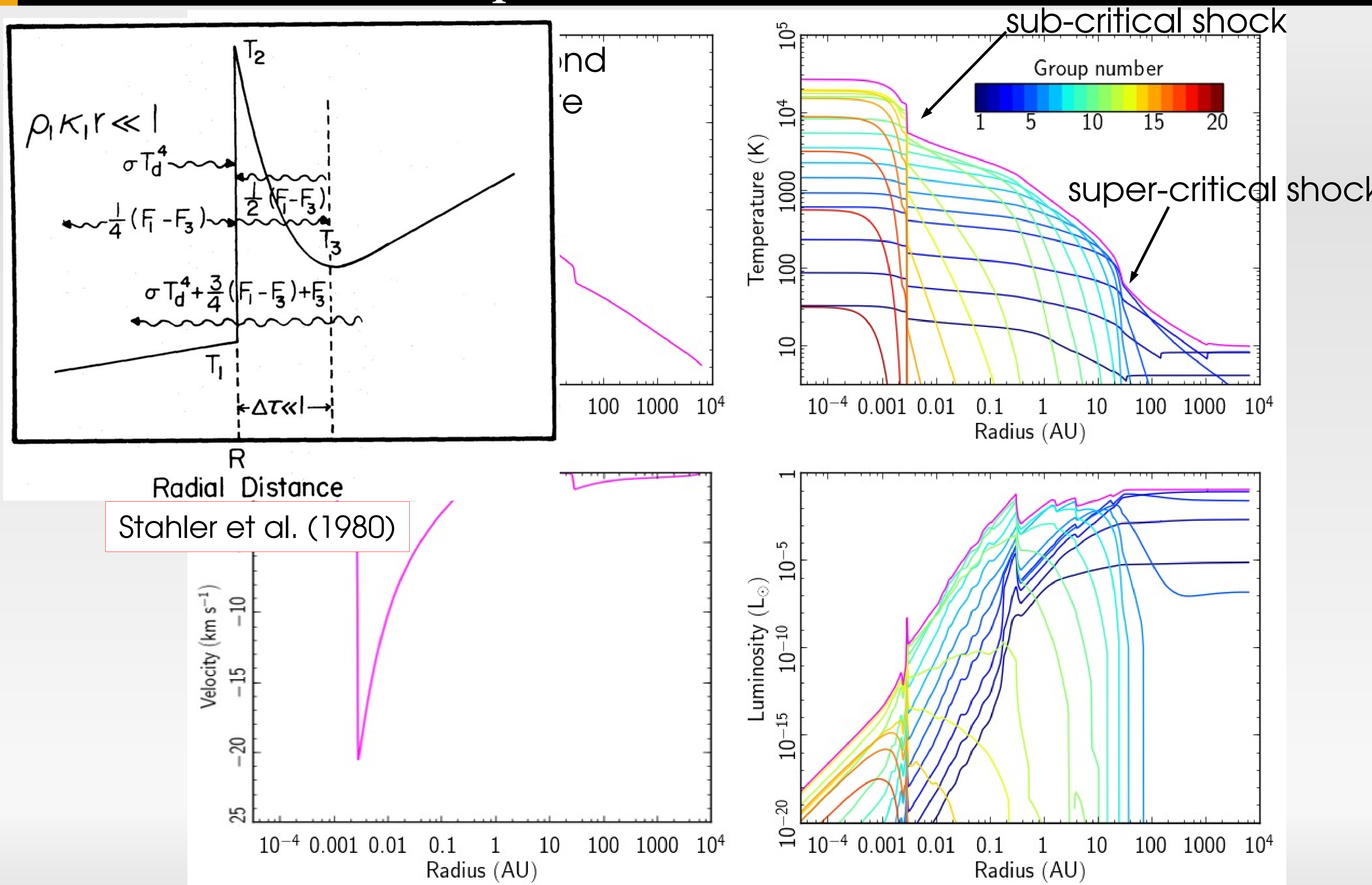

Stahler et al. (1980)

Gravitational collapse using multigroup RHD

- Results: radial profiles

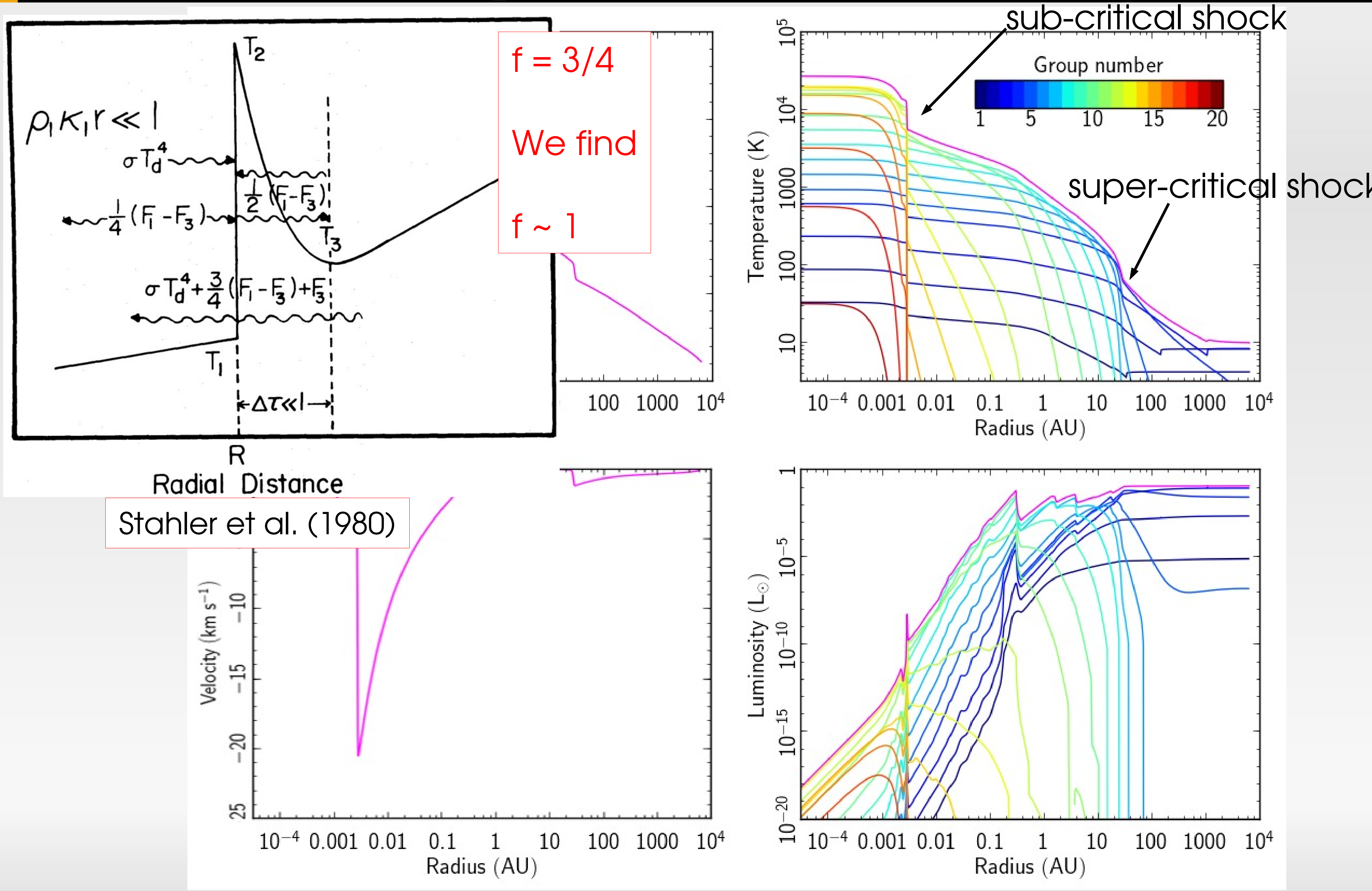

Gravitational collapse using multigroup RHD

- Results: species concentrations

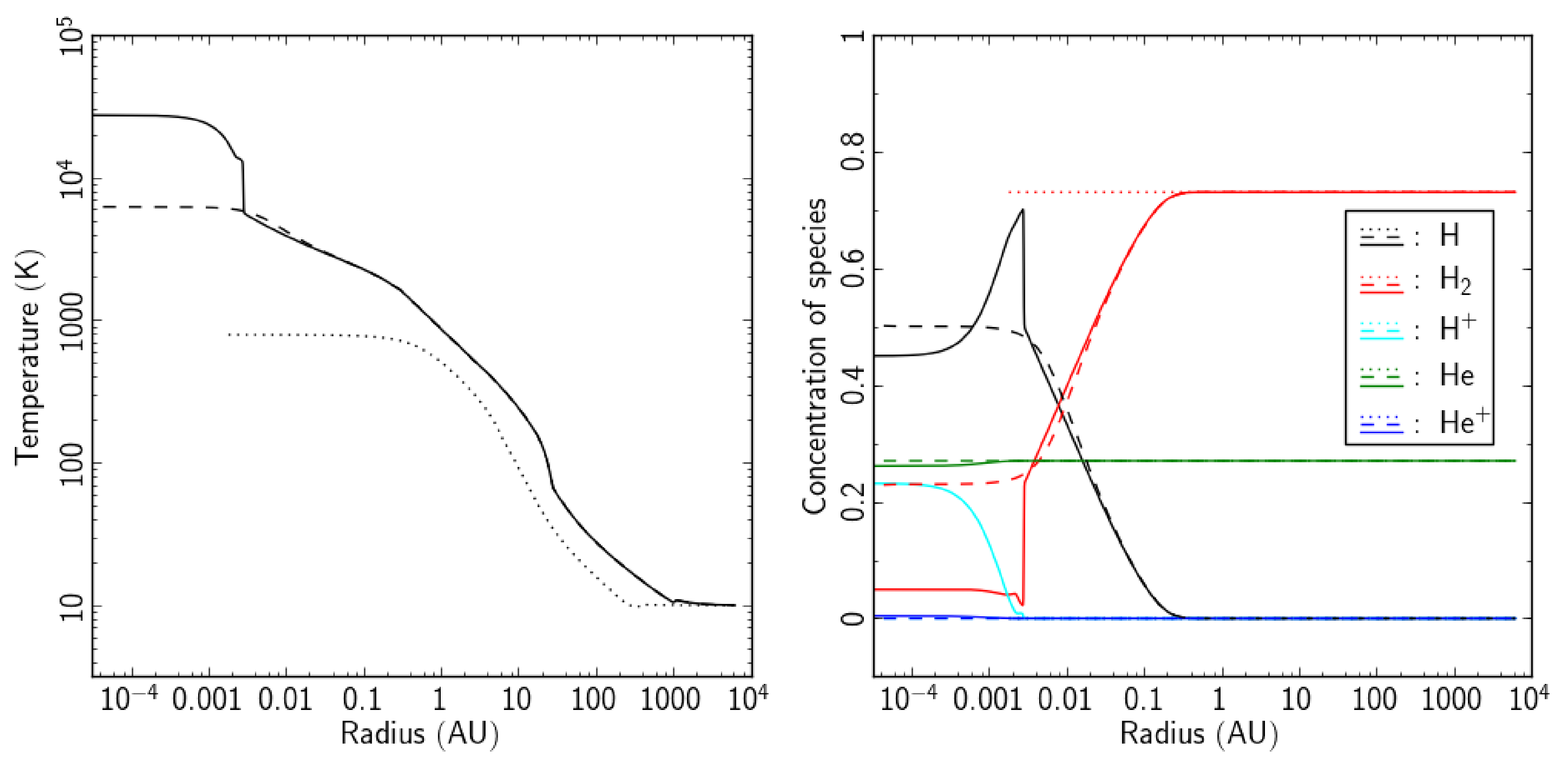

Gravitational collapse using multigroup RHD

- Results: changing the initial cloud mass

Run number	Mass of cloud	Number of groups	R_{init} (AU)	T_{init} (K)	α	t_{ff} (Myr)	Time (Myr)
1	$1\ M_\odot$	1	10^4	10	1.02	0.177	0.193
2		20					0.193
3	$0.1\ M_\odot$	1	10^3	10	1.02	0.018	0.021
4		20					0.022
5	$10\ M_\odot$	1	10^5	10	1.02	1.775	1.916
6		20					1.919
7	$1\ M_\odot$	1	5×10^3	10	0.51	0.063	0.062
8			2×10^4	5	1.02	0.502	0.551
9			10^4	5	0.51	0.177	0.177
10			5×10^3	20	1.02	0.063	0.068

Gravitational collapse using multigroup RHD

- Results: changing the initial cloud mass

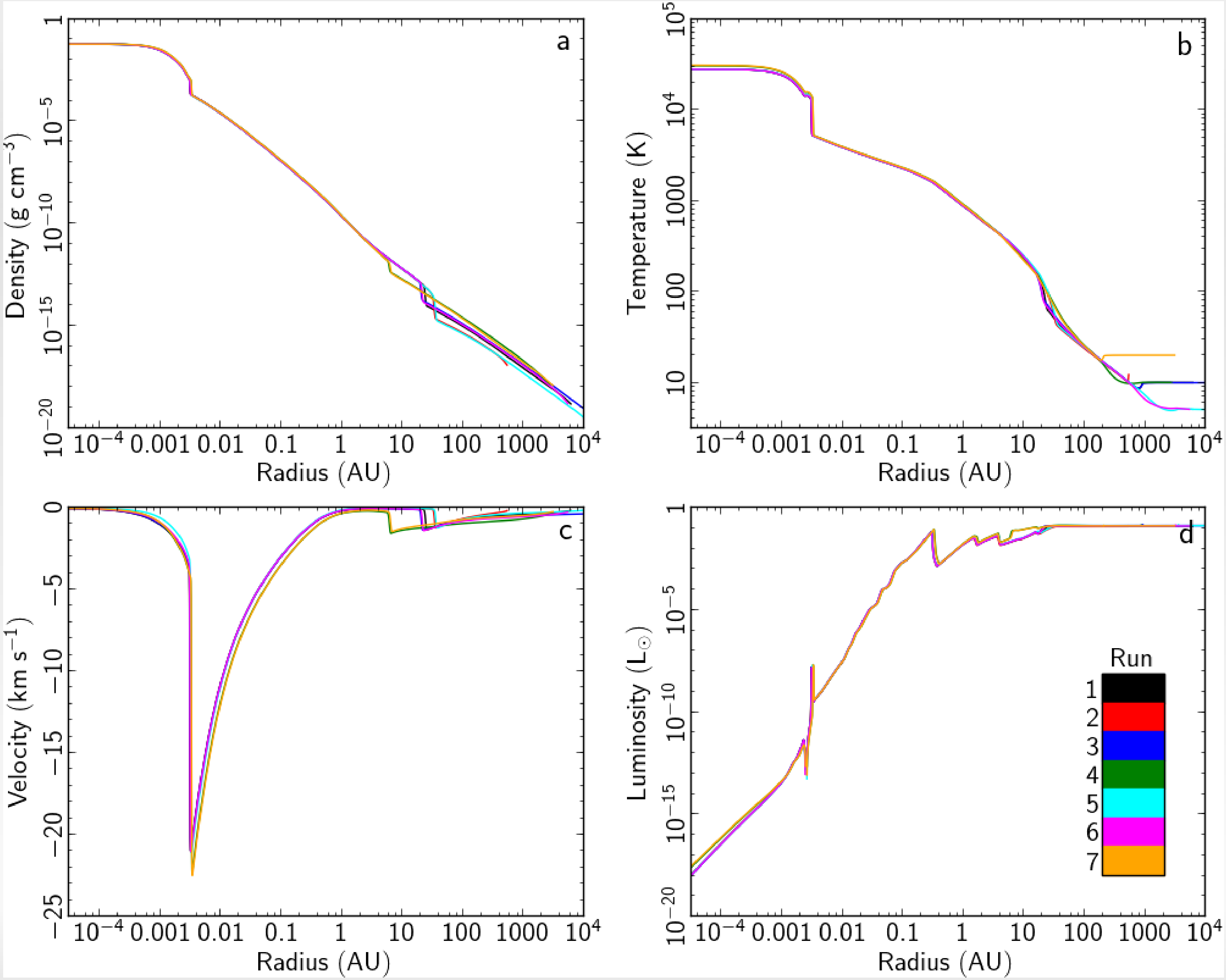

Gravitational collapse using multigroup RHD

- Results: core properties

First core										
Run number	R (AU)	M ($M_\odot$)	$\dot{M}$ ($M_\odot$/yr)	L_{acc} ($L_\odot$)	L_{rad} ($L_\odot$)	T_{fc} (K)	S_c (erg K^{-1} g^{-1})	S_N (erg K^{-1} g^{-1})	Mach number	t_{fc} (yr)
1	24.1	4.34×10^{-2}	3.53×10^{-5}	8.73×10^{-3}	1.16×10^{-1}	64	9.79×10^{8}	2.26×10^{9}	2.51	886
2	28.2	4.71×10^{-2}	3.39×10^{-5}	7.63×10^{-3}	1.09×10^{-1}	66	9.83×10^{8}	2.27×10^{9}	2.27	982
3	33.3	4.97×10^{-2}	1.49×10^{-5}	3.04×10^{-3}	1.22×10^{-1}	44	9.72×10^{8}	2.25×10^{9}	2.75	2121
4	39.6	5.36×10^{-2}	1.34×10^{-5}	2.49×10^{-3}	1.12×10^{-1}	42	9.75×10^{8}	2.25×10^{9}	2.57	2424
5	20.5	4.04×10^{-2}	4.93×10^{-5}	1.33×10^{-2}	1.15×10^{-1}	84	9.83×10^{8}	2.27×10^{9}	2.18	614
6	23.0	4.28×10^{-2}	4.88×10^{-5}	1.23×10^{-2}	1.06×10^{-1}	90	9.86×10^{8}	2.28×10^{9}	1.93	644
7	5.99	2.36×10^{-2}	1.15×10^{-4}	6.23×10^{-2}	5.65×10^{-2}	320	9.94×10^{8}	2.30×10^{9}	1.25	148
8	35.0	5.09×10^{-2}	1.35×10^{-4}	2.69×10^{-3}	1.36×10^{-1}	44	9.68×10^{8}	2.24×10^{9}	2.76	2638
9	21.2	4.08×10^{-2}	4.40×10^{-5}	1.16×10^{-2}	1.13×10^{-1}	77	9.78×10^{8}	2.26×10^{9}	2.37	763
10	6.26	2.35×10^{-2}	9.97×10^{-5}	5.10×10^{-2}	5.49×10^{-2}	304	1.00×10^{9}	2.32×10^{9}	1.20	131

Second core										
Run number	R (AU)	M ($M_\odot$)	$\dot{M}$ ($M_\odot$/yr)	L_{acc} ($L_\odot$)	L_{rad} ($L_\odot$)	T_c (K)	S_c (erg K^{-1} g^{-1})	S_N (erg K^{-1} g^{-1})	Mach number	$\mathscr{T}_{sc}$ (Gyr)
1	3.07×10^{-3}	1.34×10^{-3}	2.01×10^{-1}	1.24×10^{4}	1.61×10^{-8}	2.81×10^{4}	9.81×10^{8}	1.27×10^{9}	3.65	2.27
2	2.81×10^{-3}	1.23×10^{-3}	2.37×10^{-1}	1.47×10^{4}	5.63×10^{-9}	2.73×10^{4}	9.73×10^{8}	1.26×10^{9}	3.43	3.63
3	3.07×10^{-3}	1.34×10^{-3}	2.02×10^{-1}	1.25×10^{4}	1.52×10^{-8}	2.82×10^{4}	9.81×10^{8}	1.27×10^{9}	3.65	1.34
4	2.85×10^{-3}	1.24×10^{-3}	2.26×10^{-1}	1.39×10^{4}	6.21×10^{-9}	2.75×10^{4}	9.74×10^{8}	1.26×10^{9}	3.49	2.88
5	3.09×10^{-3}	1.34×10^{-3}	2.01×10^{-1}	1.24×10^{4}	1.71×10^{-8}	2.81×10^{4}	9.81×10^{8}	1.27×10^{9}	3.66	0.89
6	2.89×10^{-3}	1.25×10^{-3}	2.26×10^{-1}	1.40×10^{4}	8.96×10^{-9}	2.74×10^{4}	9.74×10^{8}	1.26×10^{9}	3.48	1.54
7	3.25×10^{-3}	1.53×10^{-3}	2.14×10^{-1}	1.43×10^{4}	2.15×10^{-8}	3.08×10^{4}	1.01×10^{9}	1.29×10^{9}	3.87	0.80
8	3.18×10^{-3}	1.38×10^{-3}	1.94×10^{-1}	1.20×10^{4}	1.97×10^{-8}	2.82×10^{4}	9.82×10^{8}	1.27×10^{9}	3.70	0.75
9	3.10×10^{-3}	1.35×10^{-3}	1.98×10^{-1}	1.22×10^{4}	1.53×10^{-8}	2.81×10^{4}	9.81×10^{8}	1.27×10^{9}	3.67	0.96
10	3.27×10^{-3}	1.55×10^{-3}	2.14×10^{-1}	1.44×10^{4}	2.06×10^{-8}	3.12×10^{4}	1.01×10^{9}	1.30×10^{9}	3.91	0.85

Gravitational collapse using multigroup RHD

- Results: core properties

First core										
Run number	R (AU)	M ($M_\odot$)	$\dot{M}$ ($M_\odot$/yr)	L_{acc} ($L_\odot$)	L_{rad} ($L_\odot$)	T_{fc} (K)	S_c (erg K^{-1} g^{-1})	S_N (erg K^{-1} g^{-1})	Mach number	t_{fc} (yr)
1	24.1	4.34×10^{-2}	3.53×10^{-5}	8.73×10^{-3}	1.16×10^{-1}	64	9.79×10^{8}	2.26×10^{9}	2.51	886
2	28.2	4.71×10^{-2}	3.39×10^{-5}	7.63×10^{-3}	1.09×10^{-1}	66	9.83×10^{8}	2.27×10^{9}	2.27	982
3	33.3	4.97×10^{-2}	1.49×10^{-5}	3.04×10^{-3}	1.22×10^{-1}	44	9.72×10^{8}	2.25×10^{9}	2.75	2121
4	39.6	5.36×10^{-2}	1.34×10^{-5}	2.49×10^{-3}	1.12×10^{-1}	42	9.75×10^{8}	2.25×10^{9}	2.57	2424
5	20.5	4.04×10^{-2}	4.93×10^{-5}	1.33×10^{-2}	1.15×10^{-1}	84	9.83×10^{8}	2.27×10^{9}	2.18	614
6	23.0	4.28×10^{-2}	4.88×10^{-5}	1.23×10^{-2}	1.06×10^{-1}	90	9.86×10^{8}	2.28×10^{9}	1.93	644
7	5.99	2.36×10^{-2}	1.15×10^{-4}	6.23×10^{-2}	5.65×10^{-2}	320	9.94×10^{8}	2.30×10^{9}	1.25	148
8	35.0	5.09×10^{-2}	1.35×10^{-4}	2.69×10^{-3}	1.36×10^{-1}	44	9.68×10^{8}	2.24×10^{9}	2.76	2638
9	21.2	4.08×10^{-2}	4.40×10^{-5}	1.16×10^{-2}	1.13×10^{-1}	77	9.78×10^{8}	2.26×10^{9}	2.37	763
10	6.26	2.35×10^{-2}	9.97×10^{-5}	5.10×10^{-2}	5.49×10^{-2}	304	1.00×10^{9}	2.32×10^{9}	1.20	131

Second core										
Run number	R (AU)	M ($M_\odot$)	$\dot{M}$ ($M_\odot$/yr)	L_{acc} ($L_\odot$)	L_{rad} ($L_\odot$)	T_c (K)	S_c (erg K^{-1} g^{-1})	S_N (erg K^{-1} g^{-1})	Mach number	$\mathscr{T}_{sc}$ (Gyr)
1	3.07×10^{-3}	1.34×10^{-3}	2.01×10^{-1}	1.24×10^{4}	1.61×10^{-8}	2.81×10^{4}	9.81×10^{8}	1.27×10^{9}	3.65	2.27
2	2.81×10^{-3}	1.23×10^{-3}	2.37×10^{-1}	1.47×10^{4}	5.63×10^{-9}	2.73×10^{4}	9.73×10^{8}	1.26×10^{9}	3.43	3.63
3	3.07×10^{-3}	1.34×10^{-3}	2.02×10^{-1}	1.25×10^{4}	1.52×10^{-8}	2.82×10^{4}	9.81×10^{8}	1.27×10^{9}	3.65	1.34
4	2.85×10^{-3}	1.24×10^{-3}	2.26×10^{-1}	1.39×10^{4}	6.21×10^{-9}	2.75×10^{4}	9.74×10^{8}	1.26×10^{9}	3.49	2.88
5	3.09×10^{-3}	1.34×10^{-3}	2.01×10^{-1}	1.24×10^{4}	1.71×10^{-8}	2.81×10^{4}	9.81×10^{8}	1.27×10^{9}	3.66	0.89
6	2.89×10^{-3}	1.25×10^{-3}	2.26×10^{-1}	1.40×10^{4}	8.96×10^{-9}	2.74×10^{4}	9.74×10^{8}	1.26×10^{9}	3.48	1.54
7	3.25×10^{-3}	1.53×10^{-3}	2.14×10^{-1}	1.43×10^{4}	2.15×10^{-8}	3.08×10^{4}	1.01×10^{9}	1.29×10^{9}	3.87	0.80
8	3.18×10^{-3}	1.38×10^{-3}	1.94×10^{-1}	1.20×10^{4}	1.97×10^{-8}	2.82×10^{4}	9.82×10^{8}	1.27×10^{9}	3.70	0.75
9	3.10×10^{-3}	1.35×10^{-3}	1.98×10^{-1}	1.22×10^{4}	1.53×10^{-8}	2.81×10^{4}	9.81×10^{8}	1.27×10^{9}	3.67	0.96
10	3.27×10^{-3}	1.55×10^{-3}	2.14×10^{-1}	1.44×10^{4}	2.06×10^{-8}	3.12×10^{4}	1.01×10^{9}	1.30×10^{9}	3.91	0.85

Gravitational collapse using multigroup RHD

- Results: evolution of the first core

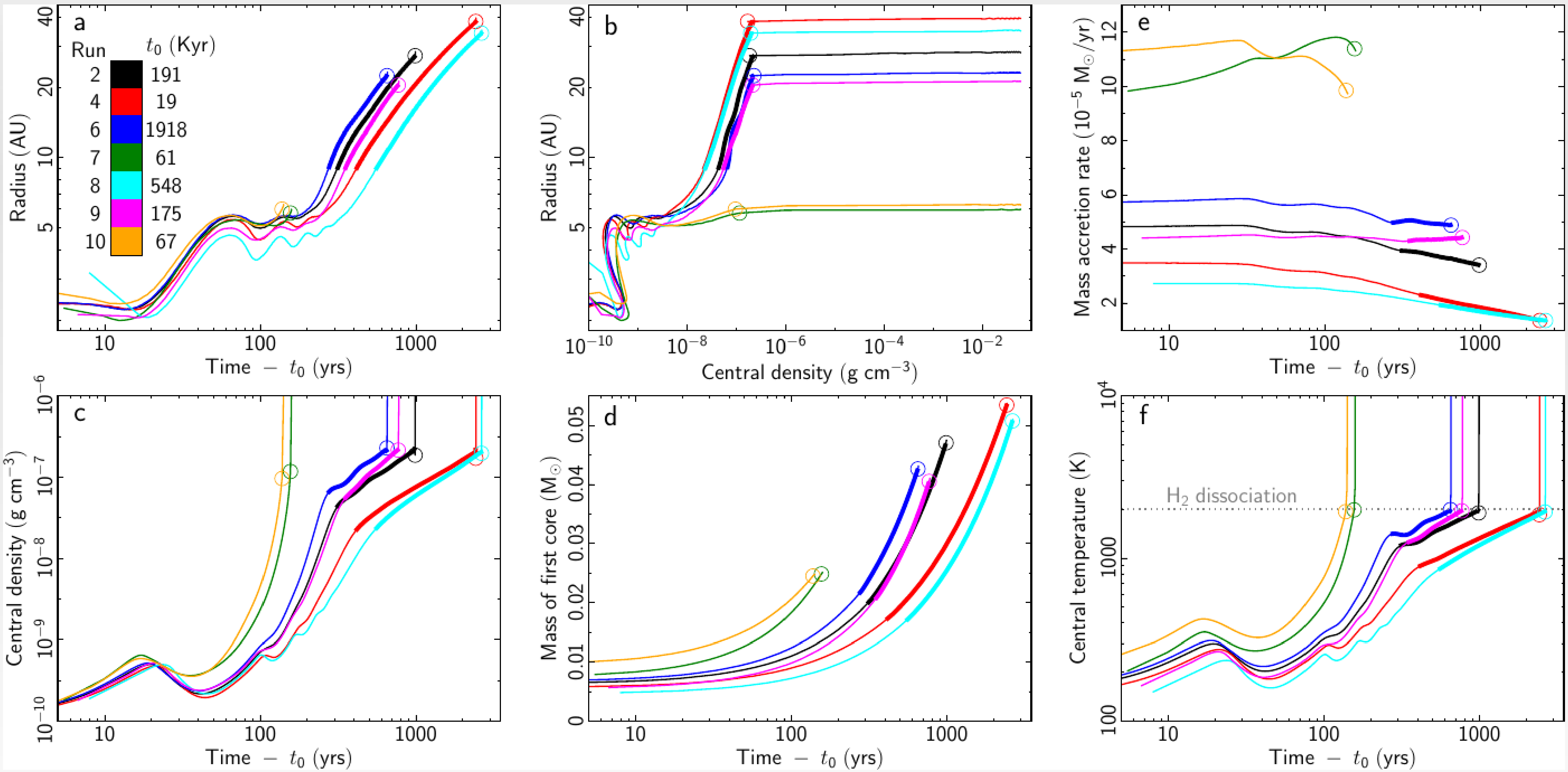

Gravitational collapse using multigroup RHD

- Results: evolution of the first core

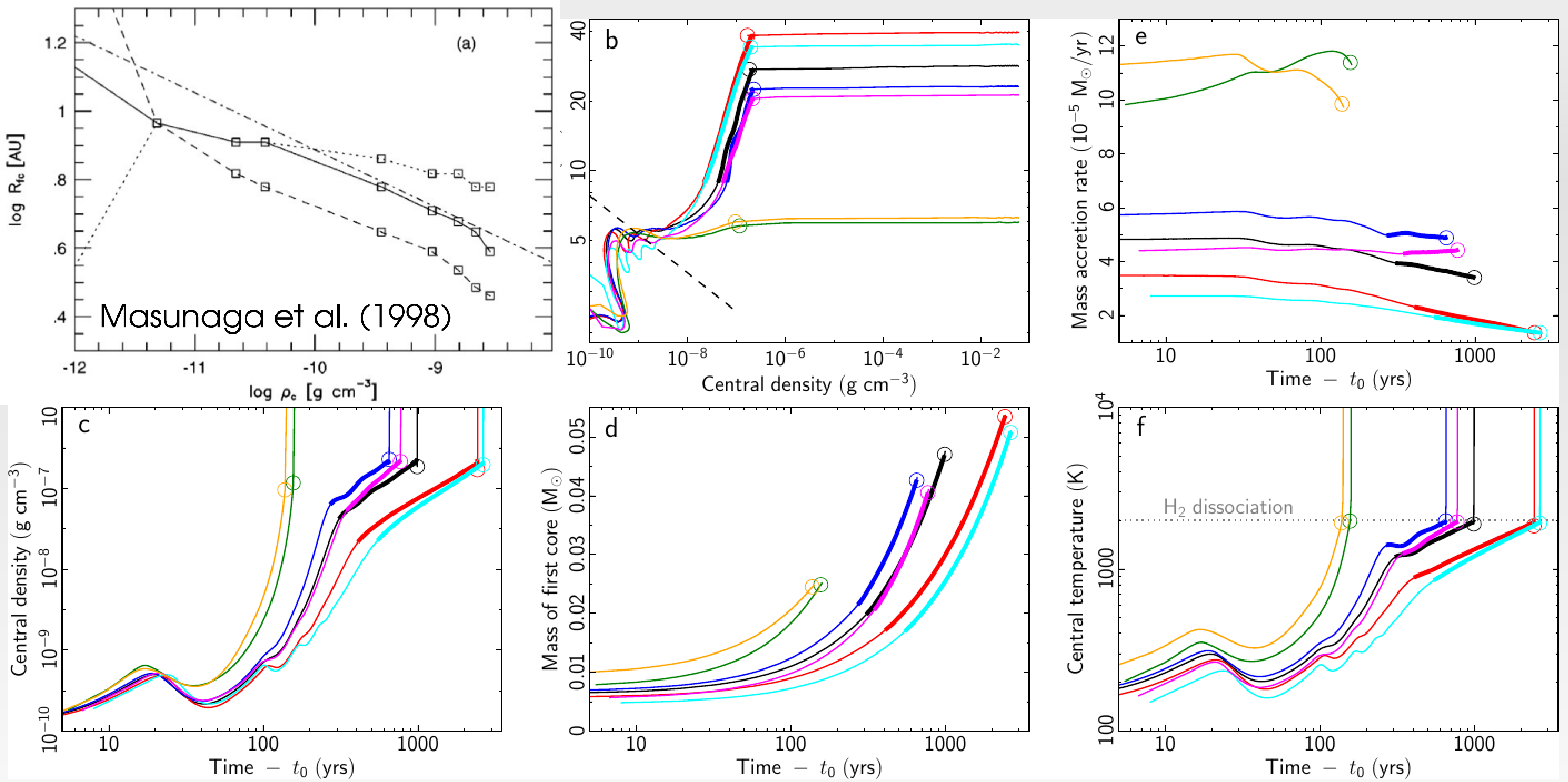

3D simulations with RAMSES – Early results

Simulations setup

Multigroup FLD + M1 in RAMSES:

- González, Vaytet, Commerçon, Masson (in prep.)
- Based on the FLD version of B. Commerçon (Ph.D. Thesis)
- BICGSTAB method
- Non-ideal MHD: ambipolar diffusion + ohmic dissipation (Masson et al. 2012, ApJS, 201, 24)

Turbulent dense cloud core:

- Cloud masses ($M_\odot$): 0.05, 0.1, 1, 3, 10, 20
- V_{rms} Mach number = 0.8 km/s × $(L/pc)^{0.4}$
- $\alpha = 5Rk_BT/2GMm_{av} = 0.3$
- Magnetization $\mu = 5$

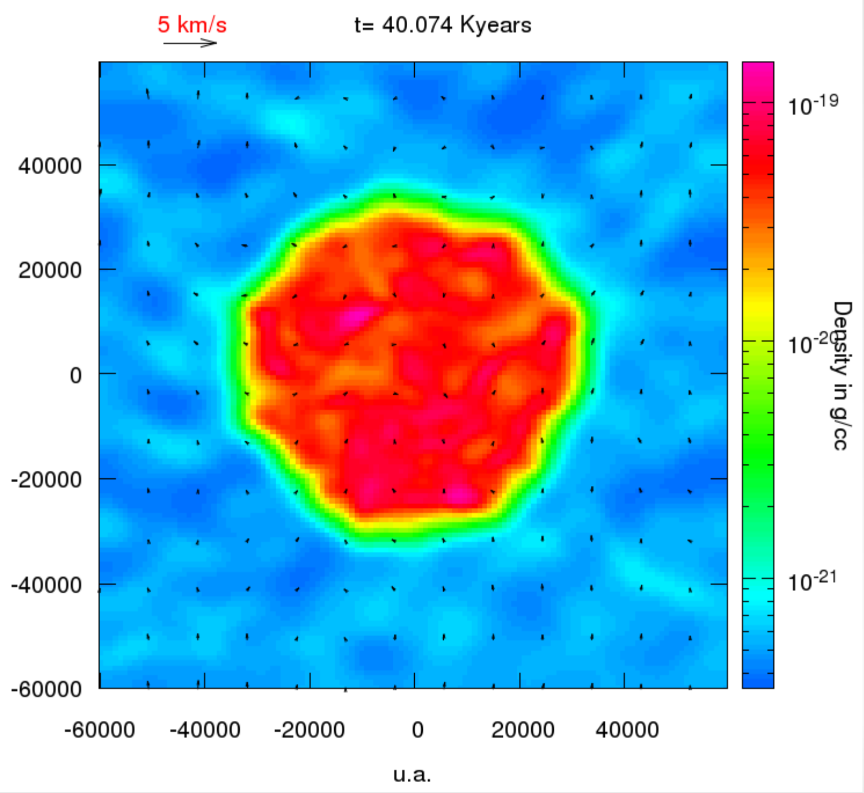

3D simulations with RAMSES – Early results

- 0.1 Msun simulation

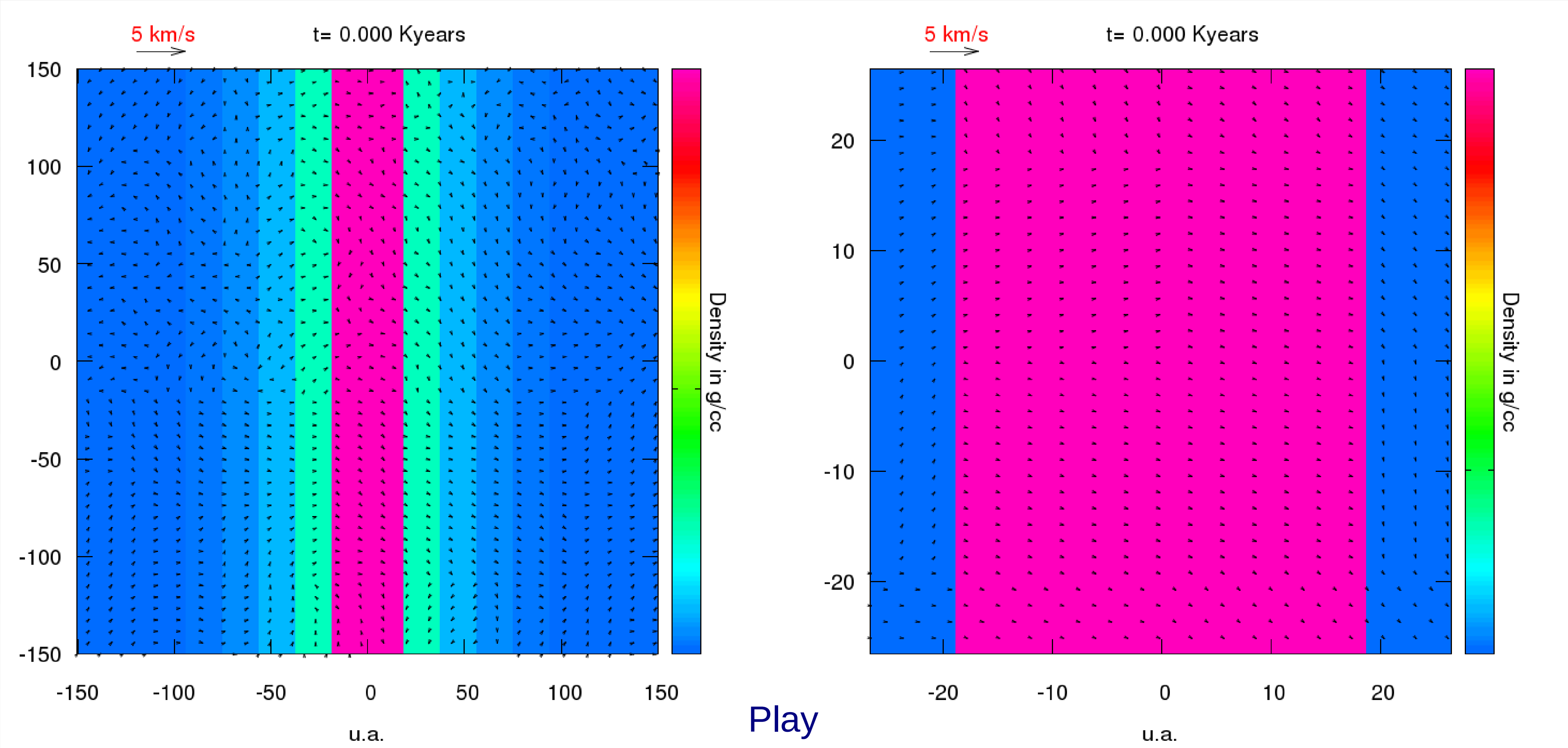

Play

3D simulations with RAMSES – Early results

- Global 200 Msun simulation + sink particles

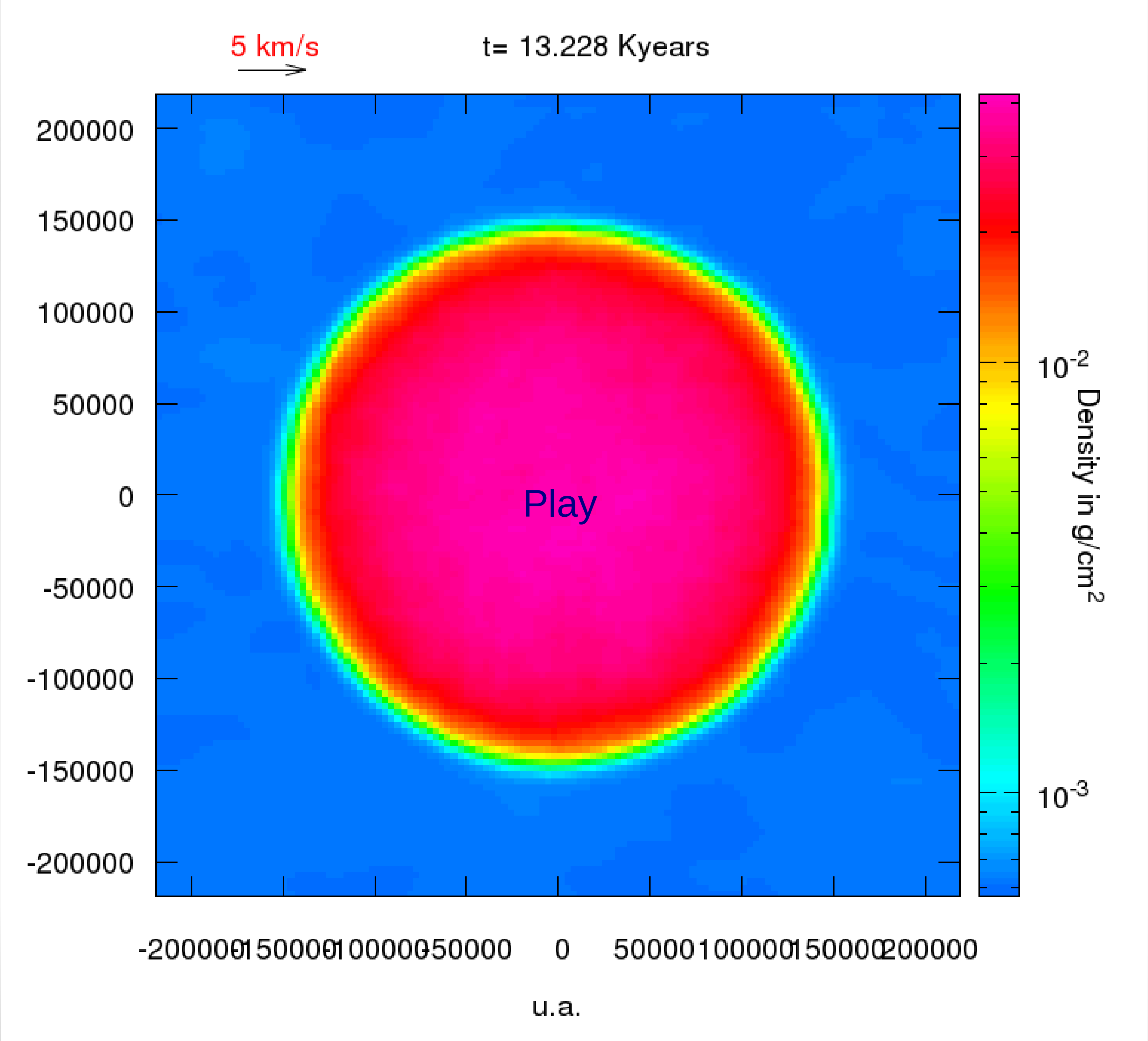

3D simulations with RAMSES – Early results

- The unwanted effects of ideal MHD: angular momentum

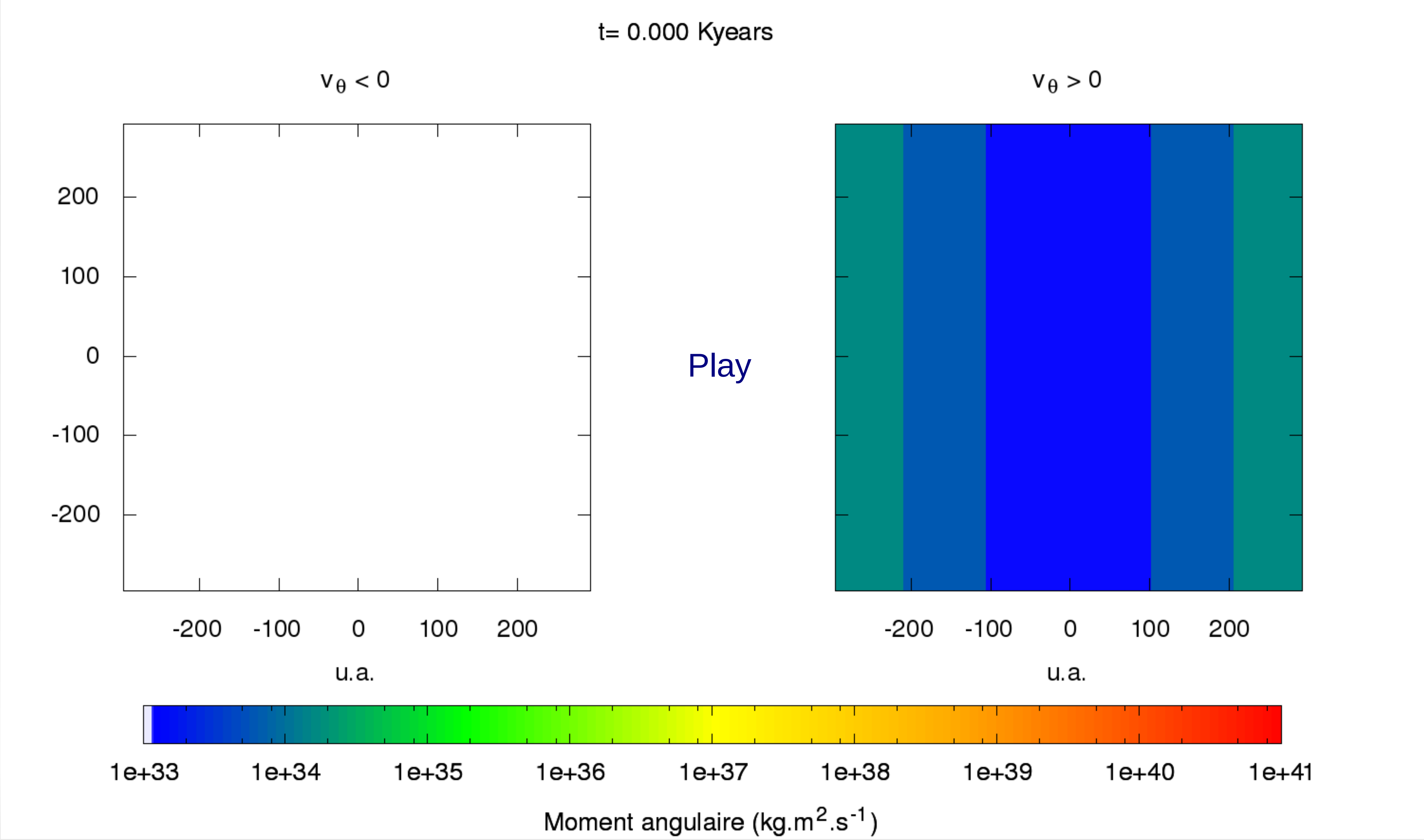

3D simulations with RAMSES – Early results

- The unwanted effects of ideal MHD: angular momentum

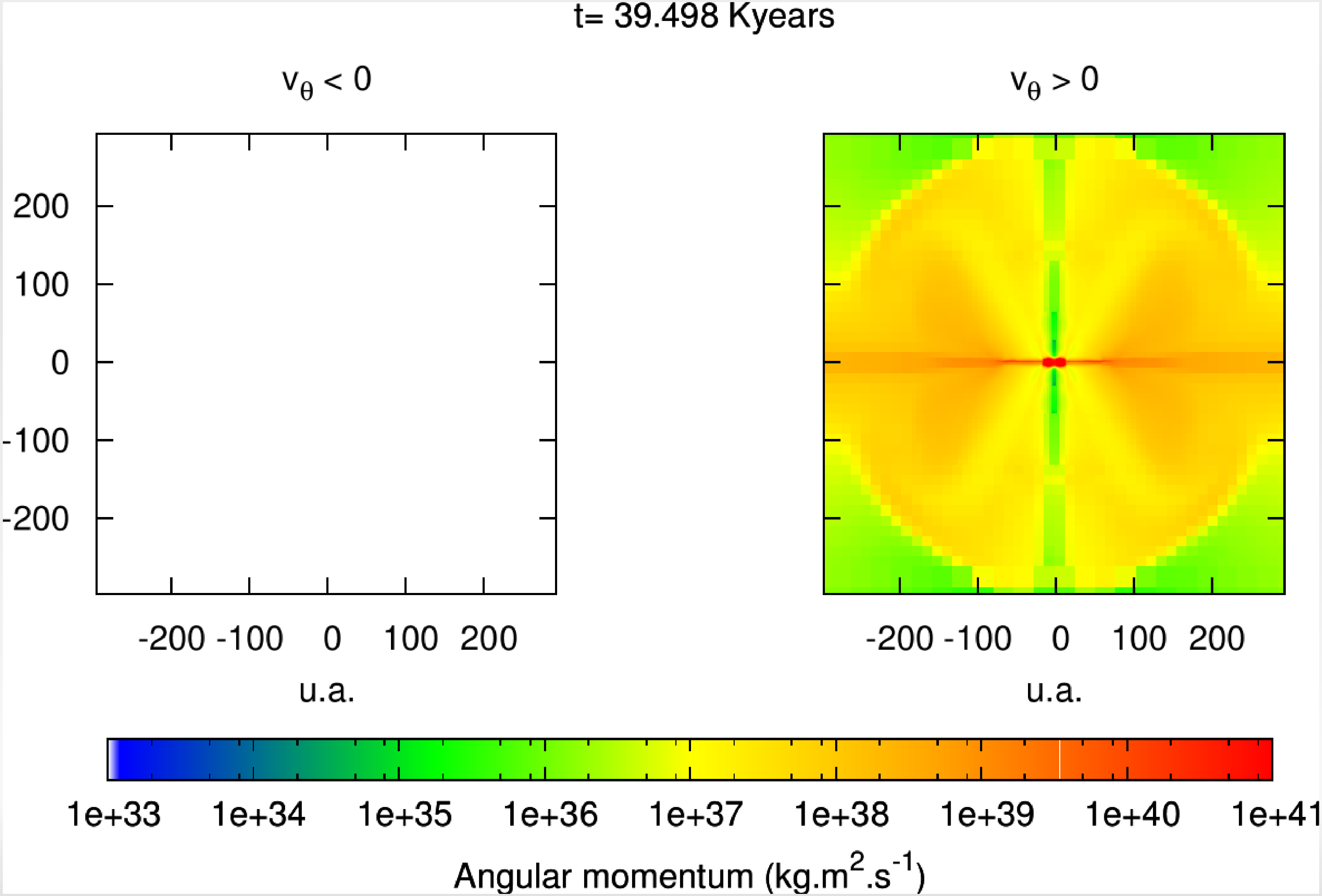

The Future?

The Future?

- FLD – M1 comparative study

Limitations of the flux-limited diffusion:

- FLD cannot reproduce shadows, radiative flux is always parallel to temperature gradient
- Disk could be shielded from stellar radiation
- This might affect fragmentation in disk

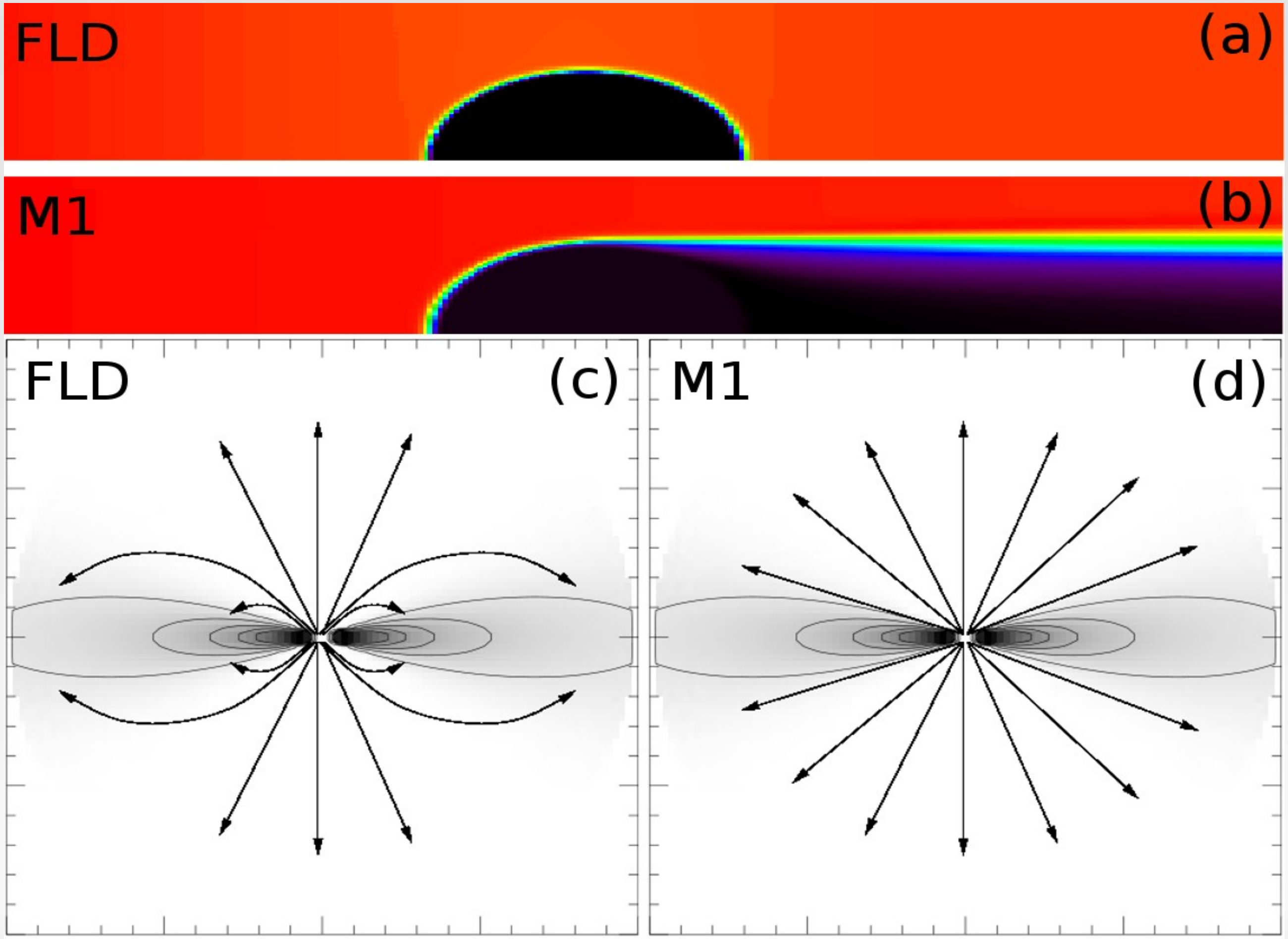

The Future?

▪ Triggering

<u>Star formation triggering with the RAMSES code</u>:

- Supernova outbursts or strong stellar radiation can trigger star formation in a nearby molecular cloud
- Efficiency is not exactly known
- 3D global simulations of triggered star formation using RAMSES with sink particles
- Provide physical insight for star formation efficiency in galaxy evolution

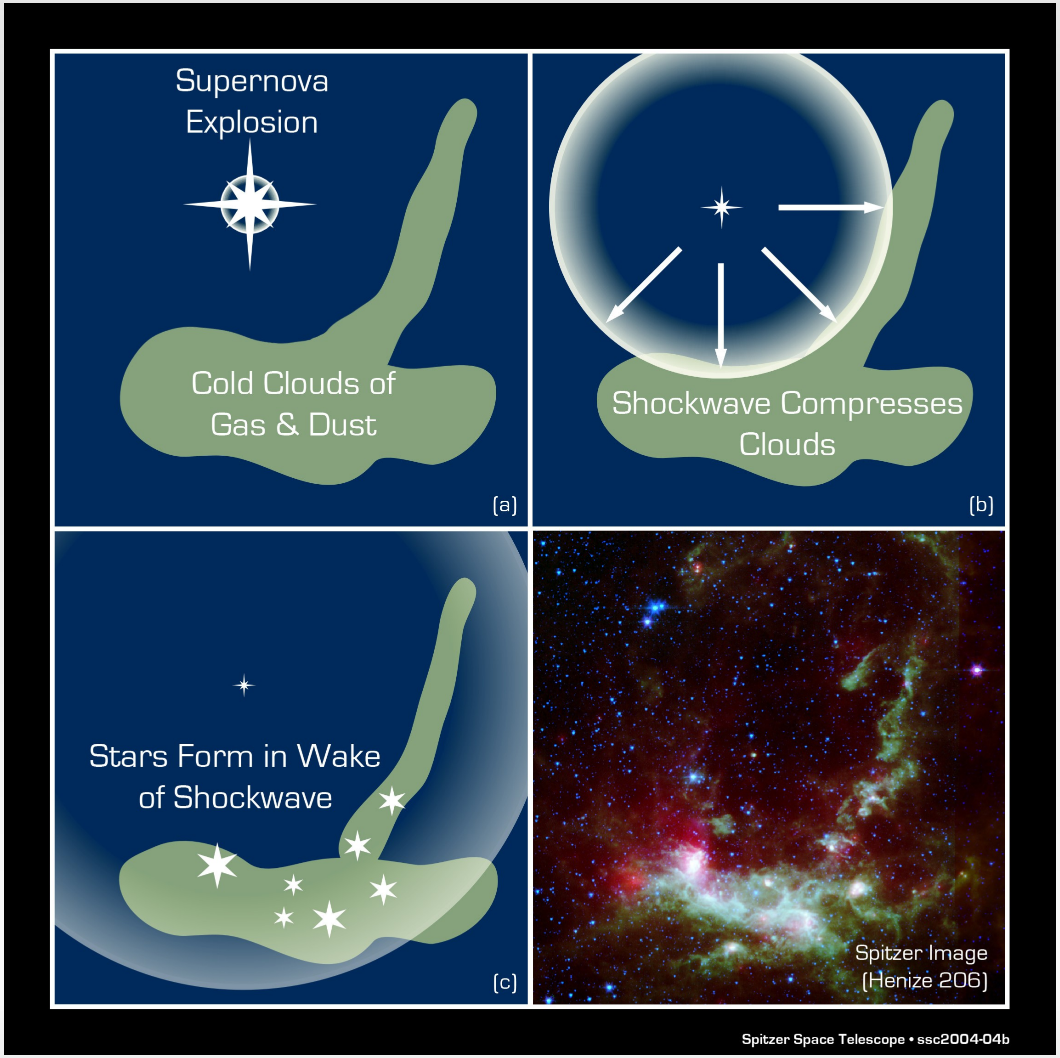

Thank you for your attention